Doctoral dissertation

Studies on non-conventional degradation pathway for *N*-glycoproteins in mammalian cells

Chengcheng Huang

Supervisor: Tadashi Suzuki

Graduate School of Science and Engineering

Saitama University

Contents

ABBREVIATIONS

BSA: bovine serum albumin

CHX: cycloheximide

CMV: cytomegalovirus

Con A: Concanavalin A

DKO: double-knockout

DIW: deionized water

Dox: doxycyclin

EDEM1: ER degradation enhancer, mannosidase α-like 1

ENGase: endo-β-*N*-acetylglucosaminidase

ERAD: endoplasmic reticulum-associated degradation

ER SP: endoplasmic reticulum signal peptide

fOSs: free oligosaccharides

Fuc: fucose

Gal: galactose

GAPDH: glyceraldehyde 3-phosphate dehydrogenase

GFP: green fluorescent protein

Glc: glucose

Gn2: glycans baring two GlcNAc at the reducing end

HRP: horseradish peroxidase

LAMP1: lysosomal-associated membrane protein 1

LC-ESI MS: Liquid chromatography–electrospray ionization mass spectrometry

LC3: microtubule-associated protein light chain 3

Man: mannose

Man2C1: cytosolic α−mannosidase

MEF: mouse embryonic fibroblast

Neu5Ac: *N*-Acetylneuraminic acid (sialic acid)

NHK: misfolded null Hong Kong α1-antitrypsin

Ngly1(PNGase): peptide:*N*-glycanase

PBS: phosphate-buffered saline

PFA: paraformaldehyde

PVDF: polyvinylidene difluoride

TCRα: T cell receptor α chain

RIPA buffer: radioimmunoprecipitation assay buffer

RTAΔ: non-toxic mutant of ricin A subunit

RTAΔm: monoglycosylated non-toxic mutant of ricin A subunit

SDS-PAGE: sodium dodecyl sulfate- polyacrylamide gel electrophoresis

Sialyl fOSs: sialyloligosaccharides (sialylated free oligosaccharide)

TBS-T: Tris-buffered saline with Tween20

TNE buffer: Tris-NaCl-EDTA Buffer

WT: wild type

SUMMARY

In eukaryotes, a large portion of the secretory and membrane proteins that synthesized in the ER are modified with asparagine-linked glycans (*N*-glycans). The covalent attachment of glycans on proteins results in changes in their physicochemical properties, as well as physiological properties.

The molecular details of the biosynthetic pathway of *N*-glycans in mammals have been well-clarified. Dolichol-linked precursors for *N*-glycans are assembled at the ER membrane and transferred to Asn residues of the consensus sequence (Asn-Xaa-Ser/Thr, Xaa≠Pro) in nascent polypeptides. The *N*-glycosylated proteins, or *N*-glycoproteins that acquired the correct folding state with the aid of various ER lumenal chaperones, are transported to their respective destinations via vesicular trafficking. Within the secretory pathway, the *N*-glycans are extensively remodeled from high mannose-type glycans to complex-type glycans that often play central roles in regulating bioactivity or stability of glycoproteins.

In contrast to the *N*-glycan biosynthesis, molecular mechanism for *N*-glycan degradation has not yet been fully understood even in mammalian cells. For instance, it has long been believed that lysosomes are the predominant organelle to break down all kinds of macromolecules including *N*-glycoproteins. However, recent studies revealed a novel non-lysosomal glycan degradation pathway occurring in the cytosol, whilst the quality

control machinery in the ER was being clarified. The ER lumen possesses quality control system that ensures only correctly folded proteins to exit the ER to their destinations, while those misfolded ones would be retrotranslocated to the cytosol for proteasomal degradation. The latter process was often called as ER-associated degradation (ERAD). During the ERAD process, a cytosolic peptide:*N*-glycanase (PNGase), which cleaves glycans from glycoproteins, initiates the non-lysosomal degradation of *N*-glycans by releasing free oligosaccharide (fOSs) in the cytosol. The released fOSs are then further processed by the action of cytosolic endo-β-*N*-acetylglucosaminidase (ENGase) that removes a single GlcNAc residue from the reducing end on the fOSs, as well as the cytosolic α-mannosidase Man2C1 before the remaining fOSs could be transported to the lysosomes for their degradation into monomeric sugars. In addition to this cytosolic glycan degradation, recent study in our lab indicated unknown functions of basal autophagy in the catabolism of complex type free glycans. These findings have shed light on the importance of non-lysosomal compartments in glycan degradation. However, detailed mechanisms underlying the non-conventional glycan degradation pathways remains largely elusive.

The purpose of my study is to elucidate the biological importance and molecular mechanisms of these glycan/glycoprotein degradation pathways. In the first chapter, I aim to clarify the physiological role of the cytosolic PNGase which works in the initial step of the non-lysosomal degradation pathway. This study is extremely important because growing number of patients showing multiple symptoms have been identified

harboring mutations in *NGLY1* (a gene encoding an orthologue of human cytosolic PNGase), while the development of therapeutic treatments is hindered due to the limited knowledge on the underlying mechanisms of the phenotypes caused by the mutation of *NGLY1* gene. Gene-knockout mice studies in our lab have revealed that the abrogation of Ngly1 (mouse PNGase) causes embryonic/perinatal lethality. Surprisingly, this lethality was rescued by an extra knockout of a gene encoding the cytosolic ENGase, clearly indicating that the presence of ENGase in *Ngly1*$^{-/-}$ mouse causes the lethal phenotype. To provide the mechanistic insight into the ENGase-caused lethality in *Ngly1*$^{-/-}$ mice, I utilized mouse embryonic fibroblast (MEF) cells derived from various knockout mice, and tried to analyze the activity of ENGase on glycoproteins in the *Ngly1*$^{-/-}$ MEF cells. Using a plant-derived glycoprotein for ERAD substrate, dysregulation of ERAD was shown in *Ngly1*$^{-/-}$ MEF cells while normal ERAD was observed in wild type, *Engase*$^{-/-}$, and *Engase*$^{-/-}$*Ngly1*$^{-/-}$ MEF cells. Moreover, a deglycosylating activity of ENGase toward a model ERAD substrate was confirmed in the absence of Ngly1, and the ENGase-generated *N*-GlcNAc containing proteins formed stable aggregates in *Ngly1*$^{-/-}$ MEF cells. Collectively, this study underscores the functional importance of Ngly1 in the ERAD process and provides a potential mechanism underlying the phenotypic consequences of a newly-emerging genetic disorder caused by mutation of human *NGLY1* gene.

In the second chapter, I aim to clarify how basal autophagy regulates the degradation of complex type free oligosaccharides. Recent observations in our lab showed that

sialyloligosaccharides, which are normally generated and degraded in the lysosomes, considerably accumulated in the cytosol of cells lacking Atg5, a molecule essential for autophagosome formation. Sialin, a sialic acid transporter in the lysosome membrane, was suggested to be somehow involved in the accumulation of sialic acid containing fOSs in *Atg5*$^{-/-}$ MEF cells. To better understand the underlying mechanisms, I examined the level of sialin molecule upon inhibition of autophagy, and the results clearly showed the increase of sialin proteins upon the inactivation of autophagy process, indicating the specific regulation of sialin by the autophagy. While the detailed mechanisms still remain to be clarified, my results clearly showed the relationship between autophagic process and stability of sialin protein.

The observations in my thesis study underscore the biological importance of the novel non-lysosomal compartment in glycan degradation, and expanded our current knowledge of the non-conventional glycoprotein degradation pathways.

INTRODUCTION

Glycans are sugars (saccharides) or sugar chains (oligosaccharides) that covalently attached to proteins/lipids or otherwise exist as a 'free', unconjugated form. Glycosylation is one of the most ubiquitous post-translational modifications of proteins in all domains of life, *i.e.* the eukarya, bacteria and archaea. The covalent attachment of glycans on proteins resulted in changes in their physicochemical properties, such as solubility or heat stability, as well as physiological properties, such as bioactivity or intra- or intercellular distribution. Different glycosylations have been identified according to the nature of the linkage to the aglycone; among them, the *N*-glycosylation or asparagine-linked glycosylation is one of the most well-studied forms of protein glycosylation.

Biosynthesis of *N*-glycoproteins

In eukaryotes, most of the secretory and membrane proteins are synthesized in the ER, and a large portion of these proteins are modified with *N*-glycans during or after their protein translation. In the ER of mammalian cells, dolichol-linked glycans comprising of fourteen sugars ($Glc_3Man_9GlcNAc_2$), namely the *N*-glycan precursor, is assembled at the ER membrane and transferred to the Asn residue in the *N*-glycosylation consensus sequence (Asn-Xaa-Ser/Thr, Xaa≠Pro) of a newly synthesized peptide by the action of oligosaccharyltransferase. The protein modified with *N*-glycans, designated hereafter as *N*-glycoproteins, would acquire proper folding in the ER, and be transported to their final destinations via the vesicular transport, with the major

population going from the ER through Golgi to plasma membrane. By the action of Golgi glycosidases and glycosyltransferases, the *N*-glycans are extensively remodeled from high mannose-type glycans, that are mainly composed of mannose (Man) and *N*-acetylglucosamine (GlcNAc), to complex-type glycans, which contain sialic acids (Neu5Ac) and galactose in addition to Man and GlcNAc[1, 2, 3]. (**Figure 1**)

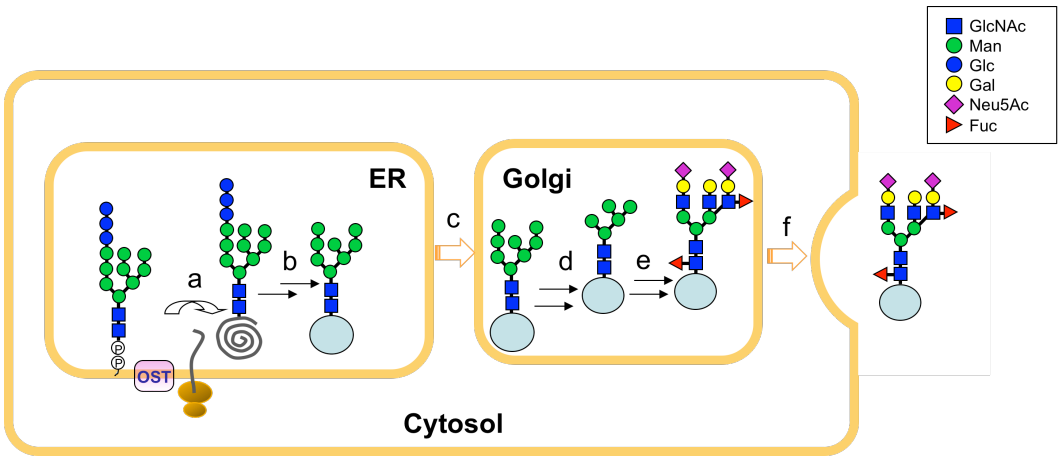

Figure 1. The biosynthesis of *N*-glycoprotein of a secretory protein. The dolichol-linked $Glc_3Man_9GlcNAc_2$ is assembled in the ER membrane and transferred to a nascent protein in the ER lumen (**a**). After folding of the protein and trimming of Glc and Man (**b**), a $Man_8GlcNAc_2$ glycan modified protein is transported to the Golgi (**c**). The Golgi mannosidases trim the glycan to $Man_5GlcNAc_2$ and various glycosyltransferases added different sugars to the glycan including Neu5Ac and Gal while passing through the secretory pathway (**d, e,** and **f**).

The conventional *N*-glycoprotein degradation in the lysosomes

The lysosomes have been recognized as the most important organelles for the cellular catabolism including glycoproteins. Two pathways work to deliver components to the lysosomes[4], both of which involves the engulfment of the substrates by a newly formed membrane and diffusion with lysosomes before the lysosomal degradation: an endocytosis process that delivers the plasma membrane proteins as well as the extra-cellular components[5, 6] (**Figure 2**), and an autophagy process that delivers cytosolic components[7, 8] (**Figure 3**). The autophagy process has been recognized as the self-eating process for the renewing of the intracellular components including large organelles. Recent studies also suggests the importance of autophagy for the proper function of lysosomes[9, 10].

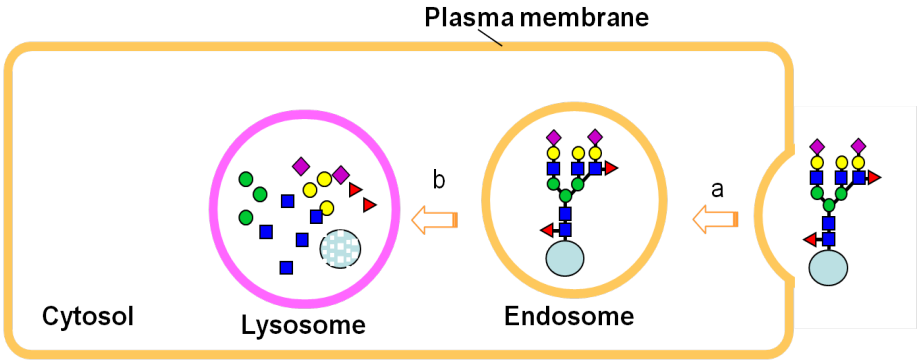

Figure 2. Degradation of a glycoprotein through endocytosis. An endosome engulfs the glycoprotein (**a**) and the endocytosed vesicle fuses with lysosome (**b**) where it is broken down into monomeric sugars and amino acids. Most of the complex type glycans are believed to be degraded through this pathway.

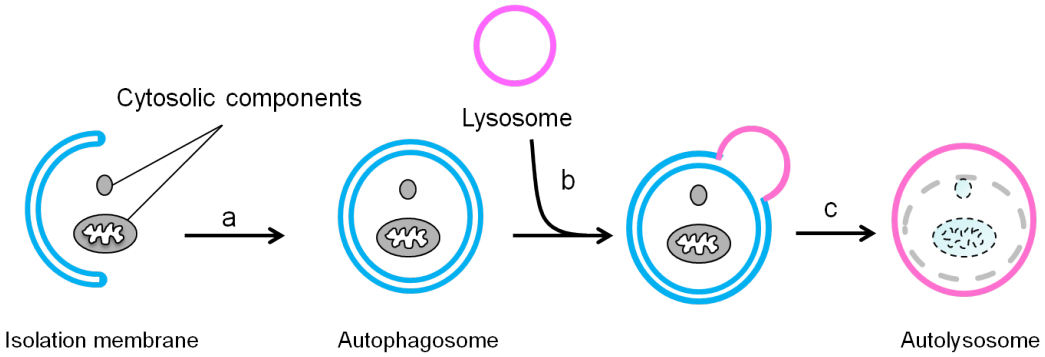

Figure 3. The process of macroautophagy (autophagy). A double-membrane structure called 'isolation membrane' in the cytosol engulfs a portion of the cytosolic components to form autophagosome (**a**); lysosomes (pink circle) fuses with the outer membrane of autophagosome (**b**) to form autolysosome and degrades the engulfed components including the inner membrane of autophagosome (**c**).

For *N*-glycoproteins that delivered to the lysosomes, proteases and various glycosidases with the characteristic acidic pH for optimal activity work bidirectionally on glycoproteins, initiated by digesting the polypeptide from the protein site, followed by dissociation of single sugars from both the non-reducing and the reducing ends in a well characterized order (**Figure 4**). The lysosomal catabolism of glycoproteins plays such important roles that mutations in glycan-degrading enzymes in the lysosomes often result in detrimental effects as are shown by some of the lysosomal storage diseases[11, 12, 13].

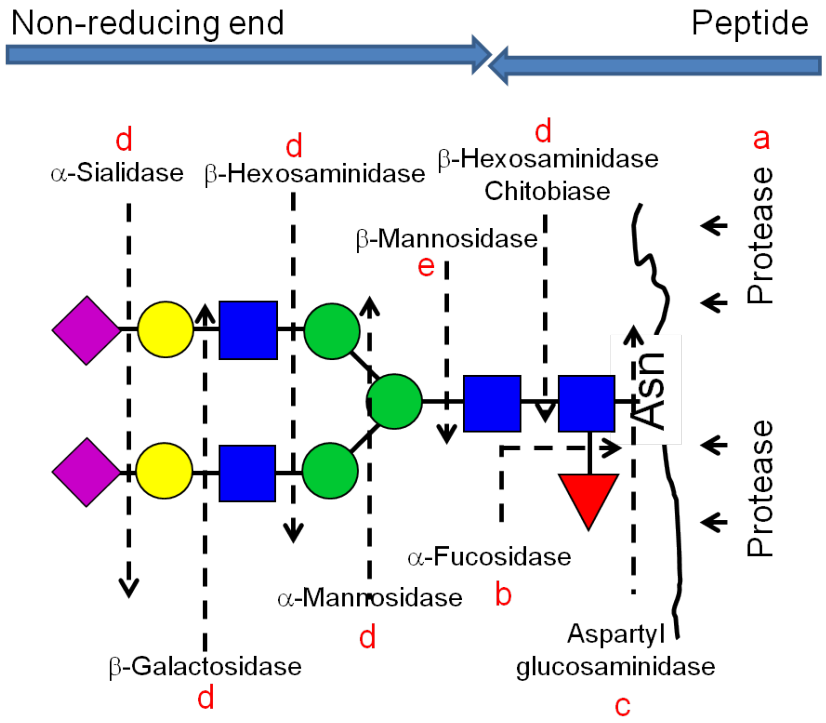

Figure 4. The lysosomal degradation of *N*-glycoprotein. (**a**) The degradation of the glycoprotein was initiated by the digestion of the polypeptide. And followed by (**b**) the removal of the terminal fucose (Fuc) by α-fucosidase; and (**c**) the cleavage between Asn and the proximal GlcNAc by an enzyme called aspartylglucosaminidase; and (**d**) the degradation of sugars from both the reducing and non-reducing ends, with chitobiase for the removal of the first GlcNAc from the reducing end, and the cleavage by α-sialidase, β-galactosidase, β-hexosaminidase and α-mannosidase in the non-reducing end in a sequential manner, with the last step by β-mannosidase. Lysosomal storage disease that caused by mutations in each glycosidases (except for chitobiase) have been identified[4, 14].

The non-conventional catabolic pathway for *N*-glycans/*N*-glycoproteins in the cytosol

The free oligosaccharides (fOSs) generated in the cytosol

While the well clarified biosynthesis as well as the lysosomal degradation of *N*-glycans/*N*-glycoproteins are carried out within the endomembrane systems, the molecular

mechanism for the generation of free *N*-glycans in the cytosol, which is segregated from the endomembrane system or extra-cellular environment by the lipid bilayer, is largely unknown.

In the cytosol of mammalian cells, high mannose-type free glycans were suggested to be generated from the ER/ER membrane by two pathways, a putative pyrophosphatase that releases glycans from dolichol linked glycans in the ER membrane to generate phosphorylated free glycans (**Figure 5 a**)[15, 16]; and Gn2 type glycans that are generated from the dolichol-linked glycan precursor by an unclarified mechanism and are transported to the cytosol by an unknown transporter (**Figure 5 b**)[17, 18]. However, the catabolism pathway for these free glycans is not known until recently. Recent studies of our lab has indicated a novel non-lysosomal degradation pathway in the cytosol for *N*-glycans that is released from the glycoproteins by a cytoplasmic deglycosylating enzyme, *i.e.* peptide:*N*-glycanase (PNGase or Ngly1) (**Figure 5 c**)[19, 20, 21, 22].

The major free glycans identified in the cytosol are high mannose type glycans originated from the ER. Recent attempts of our lab to clarify the catabolism pathway of these cytosolic free glycans, however, led to the observation of accumulated sialyl complex type glycans in the cytosol of autophagy defective cells[10], suggesting an unknown regulating mechanisms for the degradation of complex-type glycans that I would discuss in the second part (**Figure 5 g**).

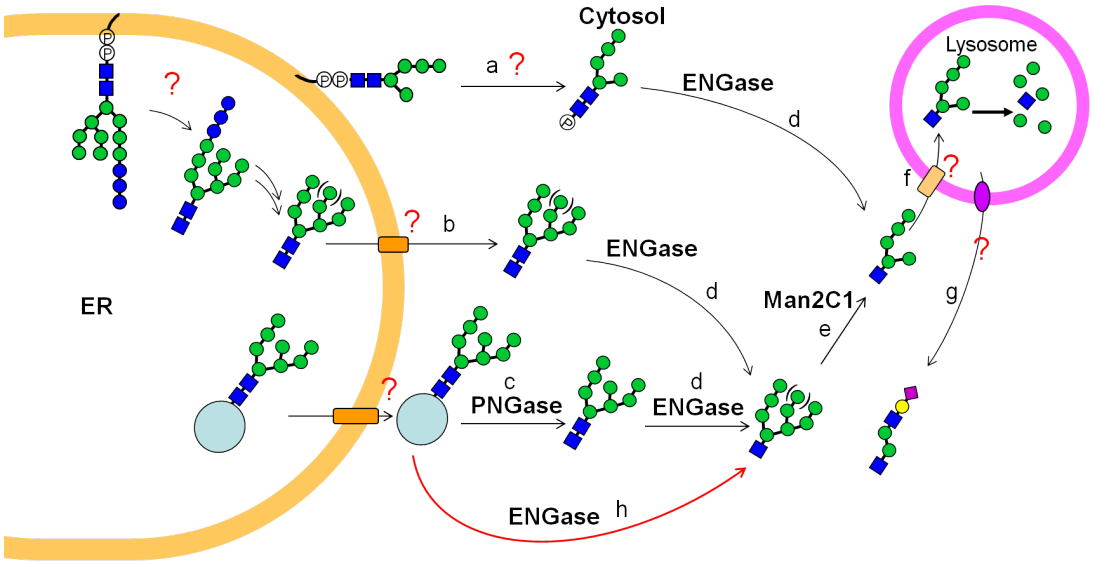

Figure 5. The non-conventional degradation pathway for *N*-glycans. Free glycans in cytosol of mammalian cells are mainly generated through three pathways. (**a**), phosphorylated free glycans are generated from a putative pyrophosphatase. (**b**), Gn2 glycans that generated in the ER are transported to the cytosol through an unknown transporter. (**c**), glycans that generated from the protein by the deglycosylating enzyme PNGase. The released glycan are further cleaved by two cytosolic enzymes, ENGase (**d**) and Man2C1 (**e**), and are processed into $Man_5GlcNAc$ before its transport to the lysosomes for final digestion. The pathway discribed in a-e are collectively referred as 'non-lysosomal degradation pathway'. Besides the high mannose type glycans, sialyl complex type glycan are released from the lysosomes by an unknown mechanism in certain conditions(**g**). In this thesis study, the ENGase mediated deglycosylation has been identified to be the forth pathway (**h**).

The non-lysosomal degradation pathway in the cytosol

The deglycosylating enzyme PNGase (peptide:*N*-glycanase; peptide-N^4-(*N*-acetyl-β-D-glucosaminyl) asparagine amidase; EC 3.5.1.52) hydrolyzes the β-aspartyl glycosylamine bond of *N*-glycopeptides/glycoproteins[23]. This enzyme was first discovered in almond[24] and subsequently in bacteria[25], and these enzymes have been

widely used as a tool reagent to analyze structures/functions of *N*-glycans on glycoproteins.

The cytosolic PNGase, first identified in mammalian cells[26, 27], has been shown to be a well-conserved enzyme throughout the eukaryotes[28]. Following the action of cytosolic PNGase, the free glycans released from the protein would further be trimmed by a cytosolic endo-β-*N*-acetylglucosaminidase (ENGase) that cleaves GlcNAc from the reducing termini of the released fOSs, followed by the action of a cytosolic α-mannosidase Man2C1, and processed glycans would finally be transported to the lysosome mainly as a $Man_5GlcNAc$ by an unknown oligosaccharide transporter on the lysosomal membrane. The glycan transferred into lysosomes are finally digested into mono-sugars in lysosomes (**Figure 5 d, e, f**)[21, 29, 30, 31, 32, 33]. These cytosolic glycan processing enzymes constitute the process called the 'non-lysosomal degradation pathway' for *N*-glycans, that is distinct from the conventional lysosomal degradation pathway.

ER-associated degradation pathway for N-glycoproteins

As the biosynthesis and conventional degradation of *N*-glycoproteins are all carried out within the vesicular systems, which is segregated from the cytosol by a lipid bilayer, it was initially very hard for scientists to understand when the localization of the mammalian PNGase was first predicted to be in the cytosol[26]. However, later the clarification of an ER-associated degradation (ERAD) made perfect sense on the cytosolic occurrence of the PNGase (see below).

The ERAD constitutes one of the quality control machineries that ensures only functional proteins to exit ER to their destinations via vesicular transport. During the ERAD process, misfolded proteins that consistently failed to acquire correct folding state would first be extracted from the ER lumen to the cytosol, a process called retrotranslocation (**Figure 6, a** and **b**), and would be targeted for proteasomal degradation (**Figure 6 d**)[34]. The cytosolic PNGase, which now has an access to these glycoproteins, is believed to play critical roles for the ERAD of glycoproteins by removing glycans from misfolded glycoproteins (**Figure 6 c**)[19, 22].

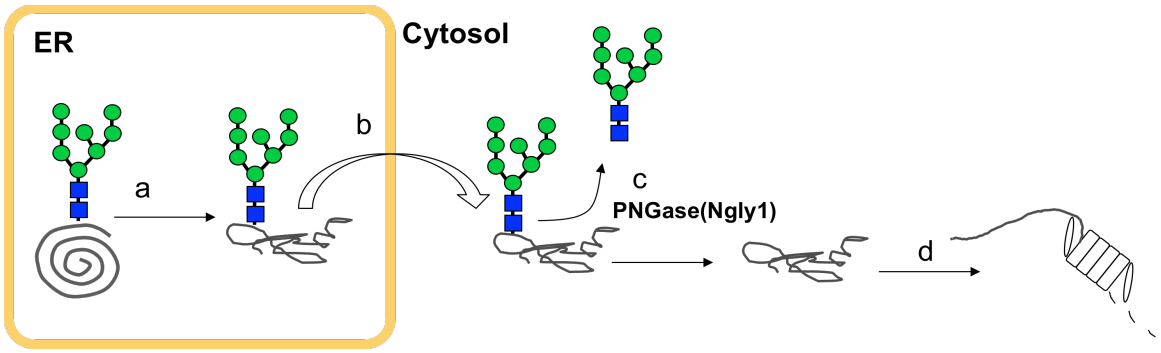

Figure 6. The ER-associated degradation pathway for *N*-glycoproteins. An *N*-glycosylated protein that constantly fails to fold properly (**a**) would be eliminated from the ER via ER-associated degradation pathway. A misfolded glycoprotein is transported to the cytosol (**b**), deglycosylated and targeted for proteasomal degradation(**c** and **d**). While the released fOSs would be further trimmed to $Man_5GlcNAc$ through the non-lysosomal degradation pathway before transported to lysosomes as indicated in **Figure 5**.

The biological significance of PNGase in different species varies a lot, for animals especially mammals, PNGase plays important biological roles according to

recent reports by us and others. In *Caenorhabditis elegans*[35], and *Drosophila melanogaster*[29], the PNGase mutant has been shown to exhibit peripheral nervous system defect and severe developmental delay, respectively. While in our unpublished knockout mice studies, the deletion of mouse PNGase orthologue, Ngly1, is embryonic/perinatal lethal (Fujihira *et al*., unpublished observation). Moreover, recent exome analysis identified patients with *NGLY1* mutation, so far twenty three patients have been identified with four deceased at early ages, showing multiple clinical features including developmental delay, abnormal tear productions, and liver malfunction[36, 37]. However, it still remains unclear how the absence of the deglycosylation enzyme causes these severe phenotypes, which also make it difficult to search for an efficient therapeutic method.

In this thesis, I focused on the novel glycan/glycoprotein degradation pathway. In the first part, my study was motivated by the surprising finding in our knockout mice study, showing that the extra knockout of the downstream glycan-processing enzyme, ENGase, rescued the lethality caused by Ngly1-knockout (Fujihira *et al*., unpublished observation). The puzzling results suggested that ENGase may not merely work on free glycans. My study utilizing mouse embryonic fibroblast cells and a model ERAD substrate gives the evidence that the cytosolic ENGase could cleave glycans from a model glycoprotein for ERAD and generate *N*-GlcNAc-modified proteins, and this action was proven to be especially evident in the absence of PNGase. In the second part, my study was based on the observation that lysosomes may release sialyloligosaccharides, *i.e.* the sialic acid containing complex type free glycans, to the cytosol when the formation of autophagosome is blocked, and the sialic acid transporter sialin was

suggested to be somehow involved in the release of sialyloligosaccharides. I aim to analyze the regulation of sialin by autophagy, and my result showed that sialin was stabilized during the autophagy deficiency, suggesting specific regulation of this lysosomal membrane transporter by autophagy.

This thesis study expanded our current knowledge of the non-conventional glycoprotein degradation pathways, while future studies must be awaited for detailed mechanisms.

Chapter 1. Functional studies of the cytosolic deglycosylating enzymes in mammalian cells

ABSTRACT

The cytoplasmic peptide:*N*-glycanase (PNGase; Ngly1 in mice) is a deglycosylating enzyme involved in the ER-associated degradation (ERAD) process. This enzyme has been shown to be indispensible for mammals, while the precise role of Ngly1 in the ERAD process remains unclear. In this chapter, to investigate the functional importance of PNGase in the ERAD, I used mouse embryonic fibroblast (MEF) cells, and showed that the ablation of Ngly1 causes the dysregulation of the ERAD process. Interestingly, not only delayed degradation but also the deglycosylation of a misfolded glycoprotein was observed in *Ngly1*$^{-/-}$ MEF cells. The unconventional deglycosylation reaction was found to be catalyzed by the cytosolic endo-β-*N*-acetylglucosaminidase (ENGase), generating aggregation-prone *N*-GlcNAc proteins. The ERAD dysregulation in cells lacking *Ngly1* was restored by the additional knockout of *Engase*. This study underscores the functional importance of Ngly1 in the ERAD process and provides a potential mechanism underlying the phenotypic consequences of a newly emerging genetic disorder caused by mutation of the human *NGLY1* gene.

INTRODUCTION

Endoplasmic reticulum-associated degradation (ERAD) constitutes one of the quality control mechanisms for newly synthesized proteins in the ER. The ERAD process involves a series of events including aberrant domain recognition, ubiquitination, translocation from the ER to the cytosol, and degradation by proteasomes. Numerous lines of evidence point to the existence of an ERAD system dedicated to *N*-linked glycoproteins; in this system, specific *N*-glycan structures dictate the folding status of client glycoproteins[38, 39]. Once glycoproteins in the ER lumen are targeted for degradation, they are retrotranslocated into the cytosol where the 26S proteasome plays a central role in their degradation[34]. During the degradation process, *N*-glycans are removed by the action of the cytoplasmic peptide:*N*-glycanase (PNGase)[40, 41, 42].

Activity of the cytoplasmic PNGase was first described in mammalian cells[26, 27], and the gene encoding cytoplasmic PNGase (*PNG1* in yeast; *Ngly1*/*NGLY1* in mice/human) is widely distributed throughout eukaryotes[28]. The functional importance of cytoplasmic PNGase in the ERAD process is evident in yeast[43, 44, 45, 46]. On the other hand, the suppression of *Ngly1* gene expression by small interference RNA in mammalian cells resulted in a reduced deglycosylation of T cell receptor α subunit (TCRα) or MHC class I heavy chain, while no significant delay in their degradation was observed[47, 48]. Moreover, Z-VAD-fmk, a pan-caspase inhibitor, was shown to inhibit cytoplasmic PNGase activity *in vivo* but it did not impede the degradation of MHC class I heavy chain[49]. Consequently,

the functional importance of the cytoplasmic PNGase remains elusive in mammalian cells.

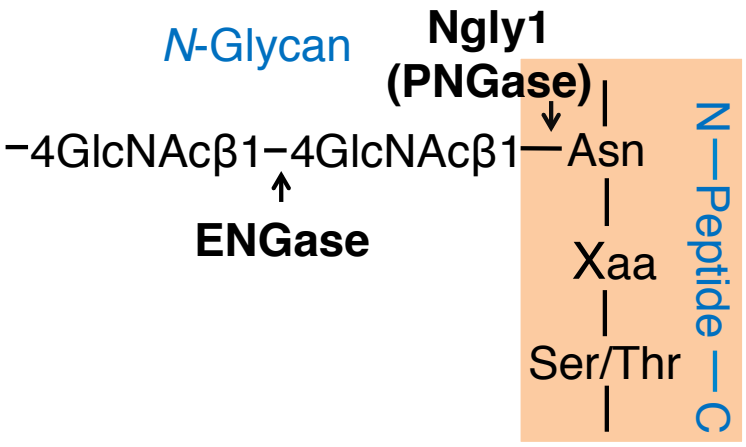

Figure 2.1 Schematic representation of the ENGase and Ngly1 (PNGase) cleavage sites on *N*-linked glycans.

PNGase-mediated deglycosylation generates free oligosaccharides in the cytosol[20]. Recent evidence suggests that a novel non-lysosomal degradation pathway exists for these cytosolic free glycans[20]. This degradation process involves cytosolic endo-β-*N*-acetylglucosaminidase (ENGase)[31, 50]. While the ENGase is believed to be involved in the catabolism of cytosolic free oligosaccharides, recent evidence shows that it can deglycosylate glycoproteins *in vivo* to generate *N*-GlcNAc-bearing proteins in *Arabidopsis thaliana*[51], raising the possibility that this enzyme may also act as a deglycosylation enzyme for misfolded glycoproteins in the cytosol[23, 52] (**Figure 2.1**).

Recently, patients harboring mutations on the *NGLY1* gene, an orthologue of the cytoplasmic PNGase in mammalian cells[53], have been described[36, 37]. While this observation emphasizes the functional importance of this protein in mammalian cells, mechanistic insight into the phenotypic consequences of these patients remains unclarified. In this chapter, I established an ERAD model substrate, RTAΔm, and demonstrated that the delay in its degradation was evident in *Ngly1*$^{-/-}$ MEF cells. Interestingly, the delay was canceled by additional gene knockout of ENGase. The degradation of RTAΔm in double-knockout cells remains proteasome-dependent, clearly indicating that the presence of an *N*-glycan on RTAΔm did not affect the efficiency of proteasomal degradation. Moreover, the occurrence of *N*-GlcNAc-modified RTAΔm in *Ngly1*$^{-/-}$ MEF cells was identified by MS analysis, demonstrating that the ENGase-mediated deglycosylation of an ERAD substrate can indeed occur *in vivo*. Interestingly, the *N*-GlcNAc protein was shown to form stable, mild detergent-insoluble protein aggregates. This study propose the critical function of *N*-glycans, maintaining the conformation/solubility of the cognate proteins destined for proteasomal degradation in the cytosol.

RESULTS

Establishment of RTAΔm as an Ngly1-dependent model glycoprotein ERAD substrate in mammalian cells

In order to provide insight into the functional significance of Ngly1 in the glycoprotein ERAD processes in mammalian cells, I aimed to establish a model ERAD substrate that could be degraded in an Ngly1-dependent fashion. Since previously our lab has established the ricin A chain non-toxic mutant (RTAΔ) as the first Png1 (yeast PNGase)-dependent ERAD substrate in yeast[43, 44], I examined whether this protein could also be degraded by a similar mechanism in mouse embryonic fibroblast (MEF) cells. To target RTAΔ to the *N*-glycosylation pathway, an ER-targeting signal peptide and an ER retention signal was introduced to the N- and C-terminus of RTAΔ, respectively (**Figure 2.2A**). RTAΔ has two potential *N*-glycosylation sites at N10 and N236 (**Figure 2.2A**), with the N10 site almost exclusively occupied by *N*-glycan in yeast[43]. To avoid any potential deglycosylation by Ngly1 or ENGase, RTAΔ was expressed in *Ngly1*$^{-/-}$*Engase*$^{-/-}$ double knockout (DKO) MEF cells and was analyzed by western blotting. As shown in **Figure 2.2B**, three bands corresponding to di-glycosylated (g2), mono-glycosylated (g1), and non-glycosylated (g0) RTAΔ were detected. To clarify which of the potential glycosylation sites were utilized, mutants for each *N*-glycosylation site were generated (N10Q and N236Q mutant; **Figure 2.2A**). As shown in **Figure 2.2B**, essentially no *N*-glycosylation was observed for the N10Q mutant, whereas N236Q is expressed mainly as a mono-glycosylated form. As expected, N10Q/N236Q mutation

resulted in the absence of glycosylated forms (**Figure 2.2B**). These results clearly suggest that N10 of RTAΔ is the main *N*-glycosylation site in mammalian cells, which is consistent with the case in yeast. For the following experiments, I utilized the mono-glycosylatable RTAΔN236Q mutant (RTAΔm) to simplify the *N*-glycosylation pattern.

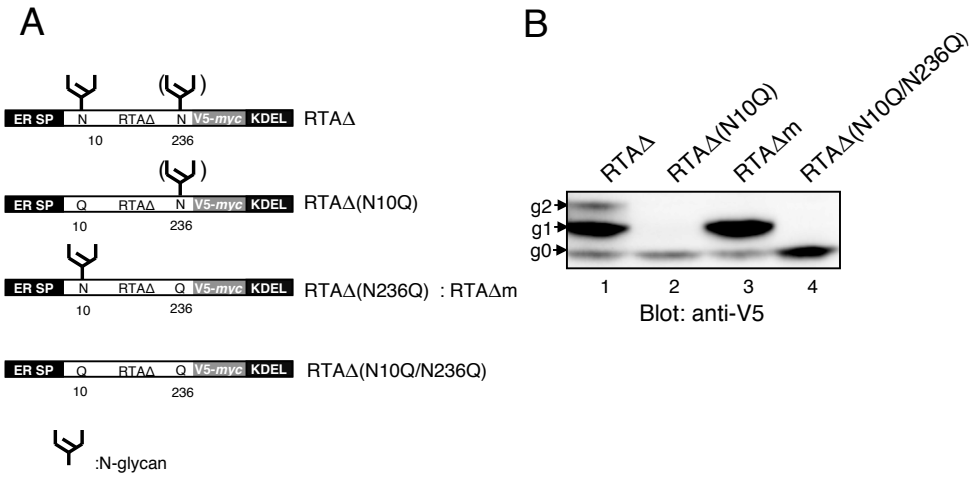

Figure 2.2 Asn10 of RTAΔ is mainly glycosylated when expressed in mouse embryonic fibroblast (MEF) cells. (A) Schematic representation of RTAΔ and its mutants used in this study. ER SP, ER signal peptide; KDEL, Lys-Asp-Glu-Leu amino acid sequence for the ER retrieval signal. N, consensus *N*-glycosylation site in RTAΔ. **(B)** Western blot analysis of various RTAΔ mutants. Extracts of *Ngly1*$^{-/-}$*Engase*$^{-/-}$ double knockout (DKO) MEF cells expressing RTAΔ, RTAΔ(N10Q), RTAΔ(N236Q)/RTAΔm, RTAΔ(N10Q/N236Q) were analyzed. g2: diglycosylated RTAΔ, g1: mono-glycosylated RTAΔ, g0: nonglycosylated RTAΔ.

When protein translation was inhibited for 3 h by a cycloheximide treatment, the amount of RTAΔm in wild type (WT) MEF cells was clearly decreased (**Figure 2.3**,

lanes 1 and 2). Moreover, the degradation of RTAΔm was inhibited by addition of MG-132, a proteasome inhibitor (**Figure 2.3,** compare lanes 2 and 4). Furthermore, proteasome inhibition resulted in an increase in the g0 form of RTAΔm, indicating the deglycosylation of RTAΔm (**Figure 2.3,** compare lanes 3 and 4). The deglycosylation of glycoprotein ERAD substrates is often observed upon treatment of mammalian cells with proteasome inhibitors[54, 55, 56, 57, 58, 59, 60]. Taken together, these results show that, as in the case of yeast[43, 44], RTAΔm is degraded by proteasomal activity and therefore can serve as an ERAD model substrate in mammalian cells.

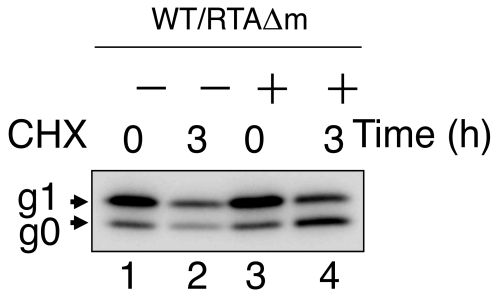

Figure 2.3. RTAΔm serves as an ERAD substrate in mouse embryonic fibroblast (MEF) cells. Effect of cycloheximide and MG-132 on the stability of RTAΔm. Each lane contains a cell extract from approximately 5×10^4 cells. Cell extracts were subjected to western blot analysis and RTAΔm was detected using anti-V5 antibody.

g0-RTAΔm is generated and stabilized in Ngly1$^{-/-}$ MEF cells

Next, I expressed RTAΔm in MEF cells derived from WT, *Engase*$^{-/-}$, *Ngly1*$^{-/-}$, and DKO mice and carried out western blotting analysis to compare the relative ratios of the g0/g1 forms of RTAΔm. In DKO MEF cells only ~10% of RTAΔm was detected as a g0 form (**Figure 2.4A,** lane 4). As DKO MEF cells do not have deglycosylating enzymes in the cytoplasm, the g0 form RTAΔm observed in DKO MEF cells must represent the

nonglycosylated form. Interestingly, when RTAΔm was expressed in *Ngly1*$^{-/-}$ MEF cells, the proportion of the g0 form (**Figure 2.4B**, column 3, 35±9%) was significantly higher than in DKO MEF cells (**Figure 2.4B**, column 4, 10±3%). Furthermore, it was noted that the g0 proportion in *Ngly1*$^{-/-}$ MEF cells was comparable to that in WT (**Figure 2.4B**, column 1, 26±10%) and *Engase*$^{-/-}$ (**Figure 2.4B**, column 2, 29±10%) MEF cells. These data strongly suggest that the deglycosylation of RTAΔm can occur independently of Ngly1 activity (**Figure 2.4A**; quantitative data in **Figure 2.4B**).

To examine the stability of RTAΔm in MEF cells, RTAΔm was expressed in MEF cells and a cycloheximide-decay experiment was carried out. The results clearly showed that, RTAΔm in *Ngly1*$^{-/-}$ MEF cells was significantly stabilized ($t_{1/2}$> 3 h) compared to WT ($t_{1/2}$=1.4±0.7 h), *Engase*$^{-/-}$ ($t_{1/2}$=1.0±0.2 h), or DKO MEF cells ($t_{1/2}$=1.4±0.5 h) (**Figures 2.4C** and **D**). The cytoplasmic PNGase-dependent ERAD of RTA-derived protein was consistent with observations in *Saccharomyces cerevisiae* [43,44]. However, it was noted that the g0 form of RTAΔm was substantially accumulated in *Ngly1*$^{-/-}$ MEF cells, which is in sharp contrast to *S. cerevisiae png1*Δ cells, where the g1 form of RTAΔ is predominantly accumulated[43,44]. While the degradation of RTAΔm in DKO MEF cells was as efficient as in WT MEF cells, its degradation remains proteasome-dependent (**Figure 2.4E**).

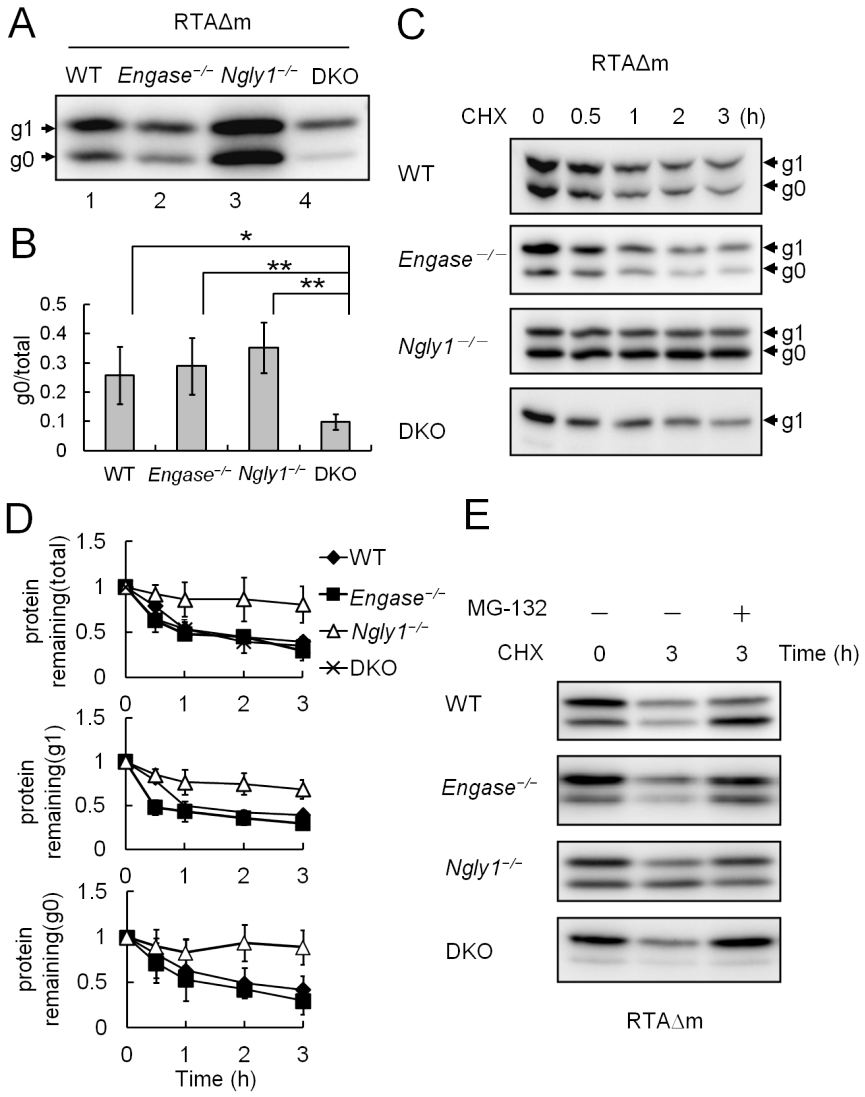

Figure 2.4. ***Ngly1***$^{-/-}$ **caused delayed degradation of RTAΔm. (A)** Western blot analysis of RTAΔm expressed in WT, *Engase*$^{-/-}$, *Ngly1*$^{-/-}$, and DKO MEF cells. Cell extracts from 5×10^4 cells (WT), 3.3×10^4 cells (*Engase*$^{-/-}$), 1.5×10^4 cells (*Ngly1*$^{-/-}$) and 2×10^4 cells (DKO) in each lane were analyzed after transfection with pEF/RTAΔN236Q/V5-*myc*/ER. **(B)** Quantification of the g0 form of RTAΔm in the four MEF cells. The data and error bars represent the average ± SD from seven independent samples. *: $p<0.05$; **: $p<0.01$; by Student's *t*-test. **(C)** Cycloheximide chase assay of RTAΔm in different MEF cells. Each lane contains approximately 5×10^4 cells and RTAΔ expression was detected using anti-V5 antibody following separation by SDS-PAGE. **(D)** (top) Quantification of RTAΔm (g1 plus g0 form). The data and error bars represent the average ± SD from at least three independent experiments. The amount of RTAΔm at the zero time point for each cell type was set to 1. (middle and bottom) Relative quantitation

of g1 (middle) and g0 (bottom) form of RTAΔm in WT, *Ngly1*$^{-/-}$ and *Engase*$^{-/-}$ cells. The amount at the zero time point for each cell type was set to 1. **(E)**, Effect of MG-132 on the stability of RTAΔm in WT, *Ngly1*$^{-/-}$, and *Engase*$^{-/-}$ and DKO MEF cells. Each lane contains a cell extract from approximately 5×10^4 cells.

Moreover, inhibiting lysosomal degradation did not cause a delay in the degradation of RTAΔm (**Figures 2.5A** and **B**). These results suggest that the presence of *N*-glycans on RTAΔm did not result in impairment in its proteasomal degradation.

In sharp contrast to the case with RTAΔm, non-glycosylated RTAΔm, which is also stabilized by MG-132 treatment and therefore can be regarded as another ERAD/proteasome substrate, was shown to be degraded in *Ngly1*$^{-/-}$ MEF cells as efficiently as in WT MEF cells (**Figures 2.5C** and **D**). This result indicates that the proteasome activity itself is not likely to be impaired in *Ngly1*$^{-/-}$ cells. Possible secondary effects due to a defect of Ngly1 to influence the experimental results, however, cannot be excluded at this point.

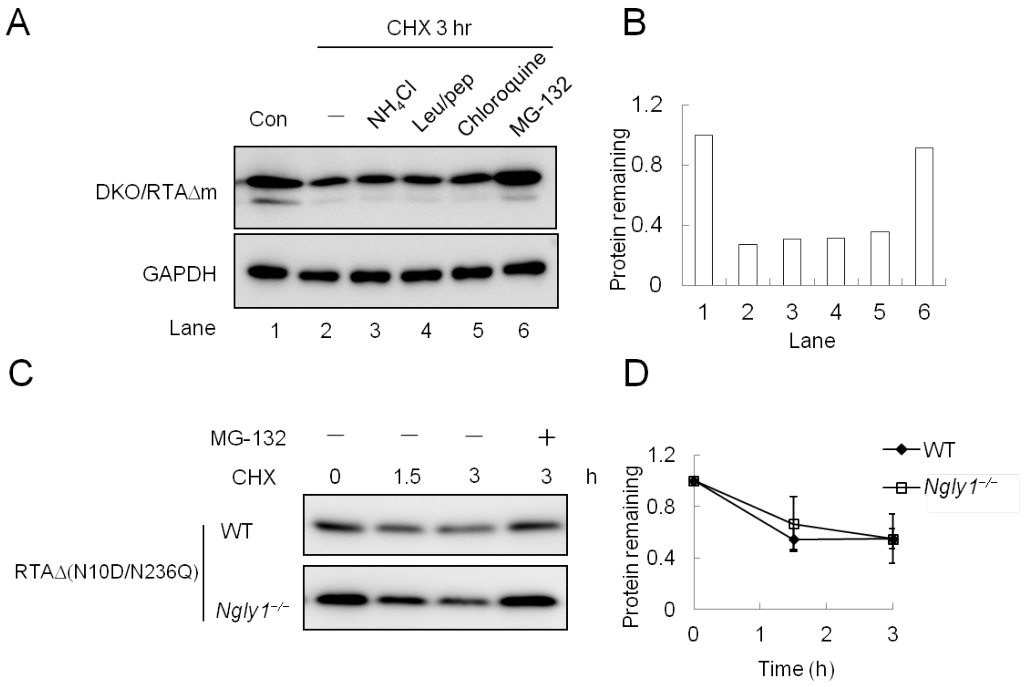

Figure 2.5. Characterization of RTAΔm degradation in various MEF cells. (A) Effect of various lysosomal inhibitors and MG-132 on the degradation of RTAΔm in DKO MEF cells. Cells transiently expressing RTAΔm were reseeded to ~60% (5×10^5 cells) confluence on 6-cm dishes and the inhibitors were added at 48 h after transfection. Each lane contains approximately 5×10^4 cells. Upper, Western blotting of RTAΔm in the presence of reagents and cycloheximide for 3 h before cell extraction. Lower, a Western blotting of GAPDH as a loading control. **(B)** Quantitation of RTAΔm shown in (A). **(C)** Cycloheximide-chase assay of RTAΔ(N10D/N236Q) (nonglycosylated RTAΔ) in WT and *Ngly1*$^{-/-}$ MEF cells . **(D)** Quantitation of data shown in (C).

ENGase generates N-GlcNAc-modified RTA⊿m, which forms RIPA insoluble aggregates in MEF cells lacking Ngly1

As *S. cerevisiae* does not contain cytoplasmic ENGase[31, 61, 62], It was assumed that in *Ngly1*$^{-/-}$ MEF cells cytoplasmic ENGase generates the g0 form of RTAΔm and that the remaining GlcNAc modification on RTAΔm results in its stability. To evaluate

whether cytoplasmic ENGase is directly involved in deglycosylation, I co-expressed ENGase and RTAΔm in DKO MEF cells. As shown in **Figure 2.6A**, the amount of the g0 form of RTAΔm was significantly higher in DKO MEF cells expressing ENGase, when compared with control (GFP-expression; **Figure 2.6A**, compare lanes 1 and 2). Interestingly, the major fractions containing g0 RTAΔm formed by ENGase-expression were not solubilized in mild detergent (RIPA buffer), indicating the formation of a RIPA insoluble aggregate (**Figure 2.6A**, lane 6). In sharp contrast, the majority of the g1 form was observed in the RIPA soluble fraction (**Figure 2.6A**, lanes 3 and 4). These results support the contention that ENGase is involved in the deglycosylation of RTAΔm and can generate an aggregation-prone g0 form of RTAΔm.

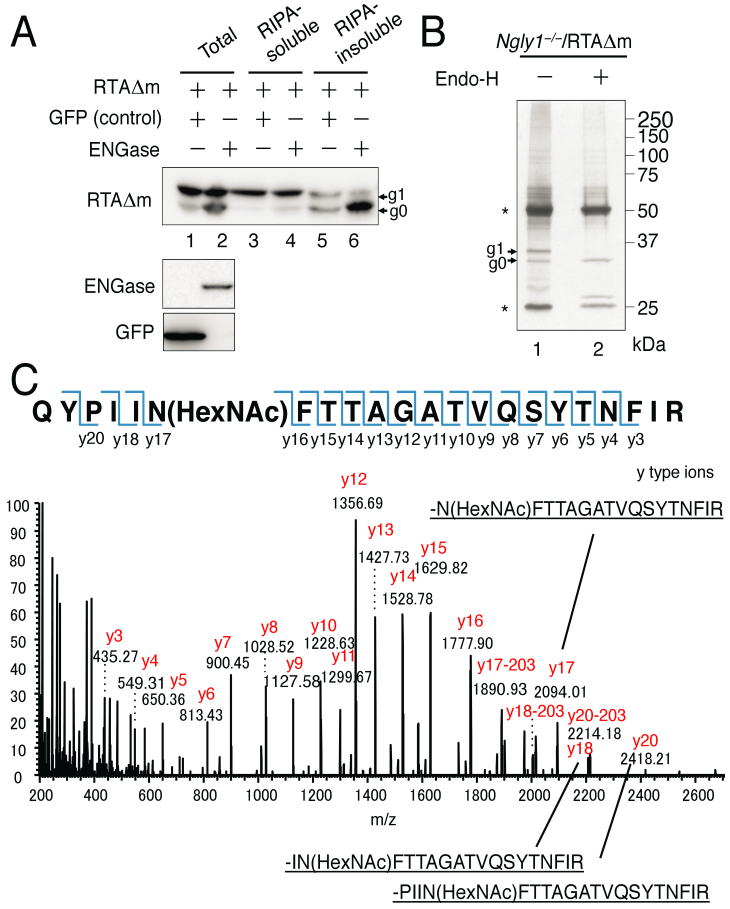

Figure 2.6. Identification of the *N*-GlcNAc modification on RTAΔm. **(A)** Co-expression of RTAΔm with ENGase results in formation of the RIPA-insoluble g0 form of RTAΔm. ENGase and RTAΔm were co-expressed in DKO MEF cells. RTAΔm and GFP co-expressing cells were used as a transfection control. Cell extracts were obtained by resuspending cells in SDS-PAGE sample buffer (lane 1 and 2; Total), or RIPA buffer (lane 3 and 4, RIPA soluble); the RIPA-insoluble fractions were solubilized using SDS-PAGE sample buffer (lane 5 and 6, RIPA insoluble). RTAΔm (upper panel) was visualized using anti-V5 antibody, while expression of ENGase (middle panel) was confirmed using anti-FLAG antibody and GFP (bottom panel) was confirmed using anti-GFP antibody. **(B)** Silver staining pattern of immunopurified RTAΔm in *Ngly1*$^{-/-}$ MEF cells. Lane 1, immunoprecipitated sample; lane 2, immunoprecipitated sample followed by Endo-H (Roche) treatment. Asterisk, antibody heavy chain (upper) and light chain (lower). **(C)** (Experiment performed by Dr. Naoshi Dohmae, Dr. Takehiro Suzuki (Collaboration Unit, RIKEN)) MS/MS spectrum of 1354.68 corresponding to a doubly charged tryptic peptide ion containing HexNAc. The mass vale of y17-y16 implies that Asn10 was modified by a HexNAc.

To further confirm the reaction product of ENGase, *N*-GlcNAc-modified RTAΔm was characterized using mass spectrometry. *Ngly1*$^{-/-}$ MEF cells stably expressing RTAΔm were treated with MG-132 for 3 h to maximize the yield of RTAΔm. Proteins were solubilized in SDS-PAGE sample buffer, and RTAΔm was immunopurified from the lysate. As shown in **Figure 2.6B**, both the g0 and g1 forms of RTAΔm were identified, and the position of g0 on SDS-PAGE was identical to the authentic Endo H-treated sample (lane 2). The g0 band of the untreated sample (lane 1) was subjected to nanoflow LC-ESI mass spectrometry (Performed by Dr. Naoshi Dohmae, Dr. Takehiro Suzuki (Collaboration Unit, RIKEN)). It was found that the peptide fragment corresponding to the *N*-GlcNAc-modified tryptic peptide (QYPIINFTTAGATVQSYTNFIR + HexNAc; see **Figure 2.7A** for the complete RTAΔm sequence) was detected at around 25.3 min in both the g0 band of the sample and the Endo H-treated authentic GlcNAc-RTAΔm sample (**Figure 2.7B**; top panel). The exact distribution pattern of isotopic ions for the peptide (top panel) was also very similar to the control (**Figure 2.7B;** bottom panel). Furthermore, the parent ion equivalent to the *N*-GlcNAc peptide was subjected to MS/MS analysis and attachment of a HexNAc residue on the N10 residue was confirmed (**Figure 2.6C**). Taken together, we can safely conclude that formation of *N*-GlcNAc modified RTAΔm by the action of ENGase can be, at least to some extent, attributed to the occurrence of the g0 form of RTAΔm in *Ngly1*$^{-/-}$ MEF cells.

A

1	IFPK**QYPIIN**	**FTTAGATVQS**	**YTNFIR**AVRG	RLTTGADVRH	EIPVLPNRVG
51	LPINQRFILV	ELSNHAELSV	TLALDVTNAY	VVGYRAGNSA	YFFHPDNQED
101	AEAITHLFTD	VQNRYTFAFG	GNYDRLEQLA	GNLRENIELG	NGPLEEAISA
151	LYYYSTGGTQ	LPTLARSFII	CIQMIFQYIE	GEMRTRIRYN	RRSAPDPSVI
201	TLENSWGRLS	TAIQESNQGA	FASPIQLQRR	QGSKFSVYDV	SILIPIIALM
251	VYRCAPPPSS	QFLEIKRGKP	IPNPLLGLDS	TAAEQKLISE	EDLNGAASEK
301	DEL				

B

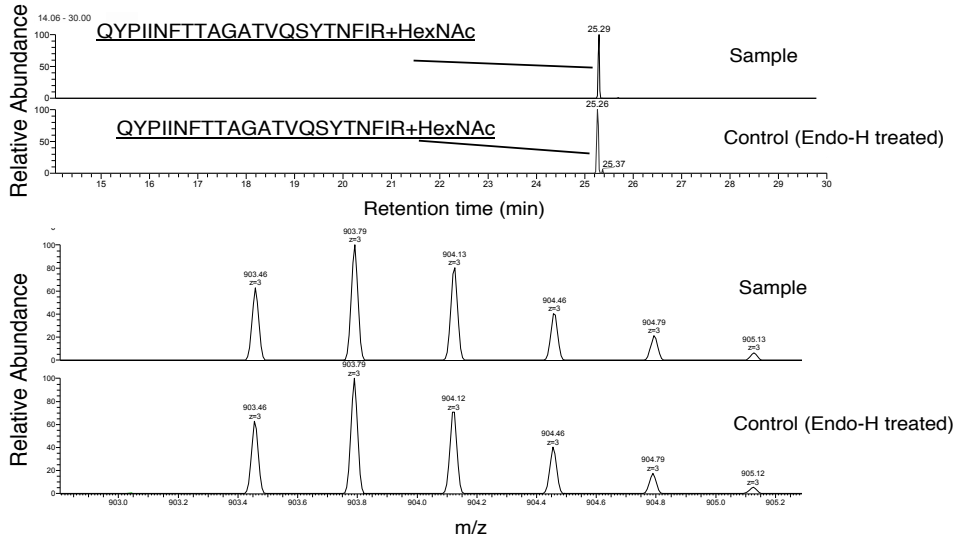

Figure 2.7. Chemical identification of *N*-GlcNAc peptide from RTAΔm. (A) Amino acid sequence of RTAΔm. Sequence from the 1st amino acid of the mature RTA was shown. The bold font sequence indicates the predicted peptide after trypsin digestion containing the N10 consensus *N*-glycosylation site (underlined). Note that Q236, originally a second *N*-glycosylation site, is now located at 231st residue due to the 5 amino acid-deletion to form non-toxic RTAΔ mutant. **(B)** (Experiment performed by Dr. Naoshi Dohmae, Dr. Takehiro Suzuki (Collaboration Unit, RIKEN).) PRM chromatogram of the QYPIIN(HexNAc)FTTAGATVQSYTNFIR peptide. Targeted ms2 product ions corresponding to y8 (1028.517), y12 (1356.691), y16 (1776.892), and y17 (2094.014) at 20 ppm mass tolerance were summed by intensity. The y8, y12, y16, and y17 product ions were extracted from ms2 mass spectra of doubly charged parent ion at 1354.68. Top: QYPIIN(HexNAc)FTTAGATVQSYTNFIR peptide detected from the g0 form of RTAΔm. Bottom: authentic QYPIIN(GlcNAc)FTTAGATVQSYTNFIR peptide from Endo-H treated sample. Lower panel, nanoflow-LC mass spectra of the eluted peptide in SIM mode; top, exact isotopic pattern of the triply charged ions of m/z 903.46 (mass value of the theoretical triply charged QYPIIN(HexNAc)FTTAGATVQSYTNFIR peptide monoisotopic ion is 903.45) observed from the g0 band; bottom, the isotopic

pattern of the authentic QYPIIN(GlcNAc)FTTAGATVQSYTNFIR peptide from an Endo-H treated sample.

Reactivity of ENGase towards misfolded glycoproteins is distinct among the possible substrates

It was noted that both g0 and g1 forms of RTAΔm were shown to be stabilized in *Ngly1*$^{-/-}$ MEF cells (**Figure 2.4D**). No significant increase in the g0 form during the chase period, however, was observed for *Ngly1*$^{-/-}$ MEF cells, even in the presence of MG-132, suggesting that ENGase-mediated deglycosylation is not as efficient as Ngly1-mediated deglycosylation (**Figures 2.8A** and **B**). In sharp contrast, an increase in the g0 form during the 3 h-chase was evident upon MG-132 incubation in WT MEF cells (**Figure 2.4E; Figures 2.8A** and **B**).

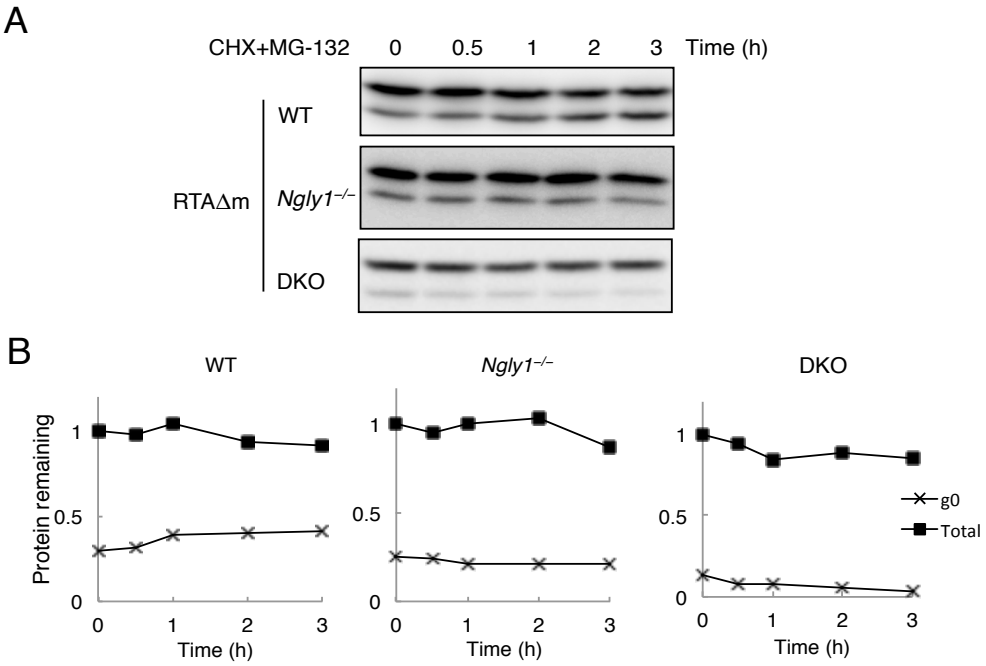

Figure 2.8. Cycloheximide chase assay of RTAΔm in different MEF cells in the presence of MG-132. (A) Cells transiently expressing RTAΔm were reseeded to ~60% (5×10^5 cells) confluence on 6-cm dishes. CHX (final concentration, 50 μg/mL) and MG-132 (final concentration, 5 μM) were then added to cells at 48 h after transfection. Each lane contains approximately 5×10^4 cells and RTAΔ expression was detected using anti-V5 antibody following separation by SDS-PAGE. **(B)** Quantitation of RTAΔm (g0 and total) shown in (A). The total amount of RTAΔm observed at zero time point was set to 1.

To obtain deeper insights into the generality of the ENGase-mediated deglycosylation of ERAD substrates, the deglycosylation status of other glycoprotein ERAD model substrates, such as the T Cell Receptor α subunit (TCRα) or the null Hong Kong variant of α1-antitrypsin (NHK), was examined. As shown in **Figures 2.9A** and **B**, in both cases the formation of a deglycosylated protein was evident, especially in the presence of the proteasomal inhibitor, MG-132 (**Figure 2.9A** lane 4; **Figure 2.9B** lane 8 at the position of the red arrows) in WT MEF cells, but with less efficiency compared to the case of RTAΔm (**Figures 2.4A** and **B**). Deglycosylated bands were not observed for DKO MEF cells, clearly indicating that they were most likely formed by the action of Ngly1 and/or ENGase. Interestingly, a protein band corresponding to deglycosylated TCRα was observed for *Engase*$^{-/-}$ and WT MEF cells, while it was not observed for *Ngly1*$^{-/-}$ MEF cells, suggesting that Ngly1 is the predominant deglycosylating enzyme for TCRα. On the other hand, the presence of deglycosylated NHK was clearly observed in *Ngly1*$^{-/-}$ and WT MEF cells, while it was somewhat less obvious in *Engase*$^{-/-}$ MEF cells (**Figure 2.9B**). In the presence of MG-132, the ratio of deglycosylated/total proteins was found to be similar between WT, *Ngly1*$^{-/-}$, and *Engase*$^{-/-}$ MEF cells, implying that

both enzymes act on NHK with similar efficiency (**Figures 2.9C**). Collectively, these results imply that the susceptibility of misfolded glycoproteins towards cytoplasmic PNGase/ENGase is distinct among the possible substrates.

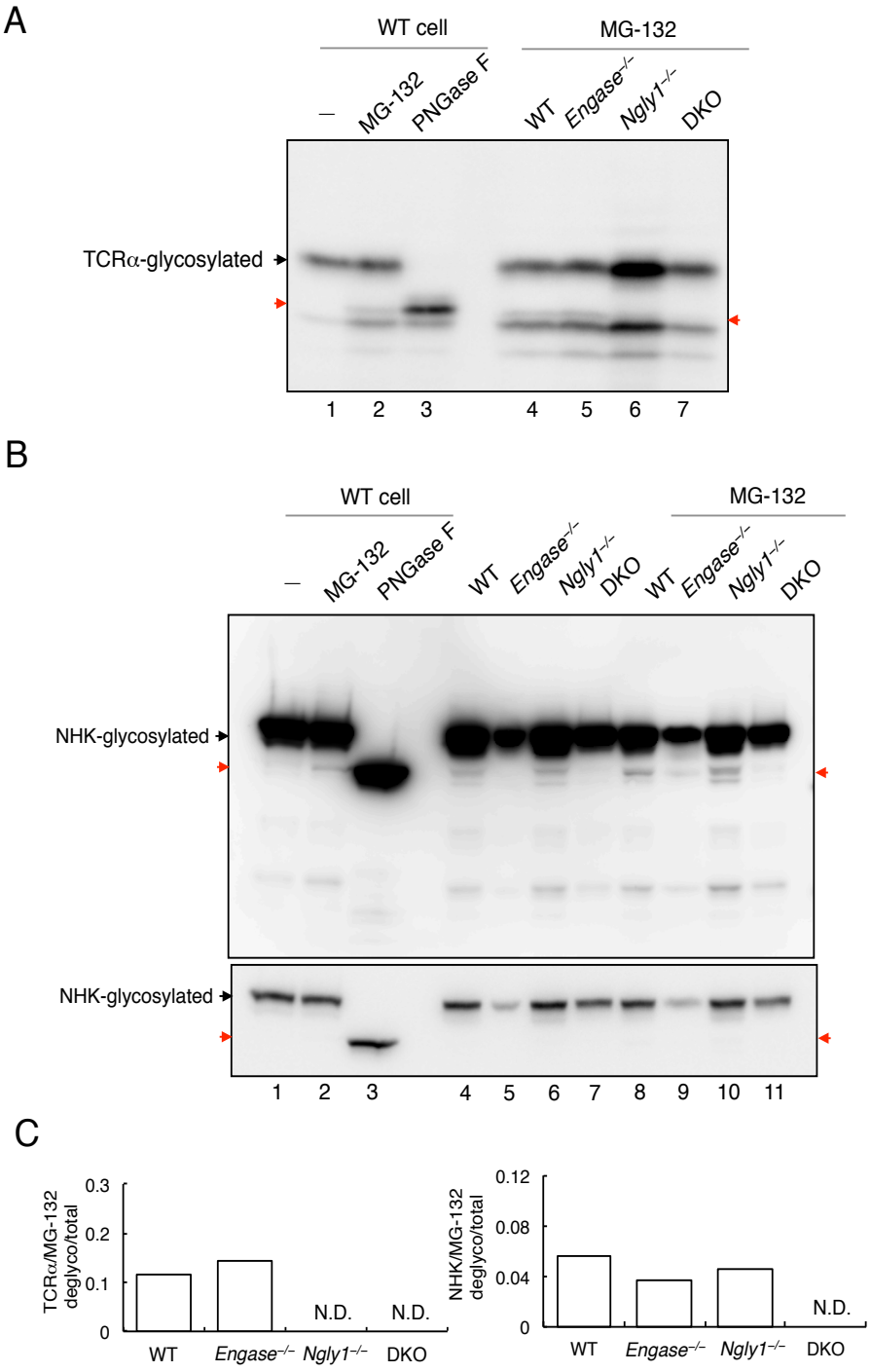

Figure 2.9. Detection of ENGase-mediated deglycosylation using model ERAD substrates. Cell transiently expressed with ERAD substrates were cultured with or without MG-132 for 3 h. **(A)** Western blotting of T cell receptor α subunit (TCRα) in

different MEF cells. Lanes 1 to 3, the confirmation of the deglycosylated TCRα in WT MEF cells. The red arrow indicates the position of deglycosylated TCRα. The occurrence of deglycosylated TCRα was evident in WT and *Engase*$^{-/-}$ MEF cells (lanes 4 and 5), but it was not detected in *Ngly1*$^{-/-}$ and DKO MEF cells (lanes 6 and 7). **(B)** (upper) Western blotting of the null Hong Kong (NHK) variant of α1-antitrypsin in different MEF cells. Lanes 1 to 3, the confirmation of the deglycosylated NHK in WT MEF cells. Red arrows indicate the position of the deglycosylated NHK. The occurrence of deglycosylated NHK in WT and *Ngly1*$^{-/-}$ MEF cells were evident with or without MG-132 treatment (lanes 4, 6, 8 and 10), while its occurrence is only apparent in *Engase*$^{-/-}$ MEF cells only when cells were incubated with MG-132 (lane 9). (lower) Short exposure of the same gel shown in upper panel. **(C)** Quantitation of the ratio of deglycosylated/total protein shown in (A) and (B). N.D.: not detected.

Higher levels of cytosolic N-glycoproteins were observed in Ngly1$^{-/-}$Engase$^{-/-}$ double KO MEF cells

While the deglycosylation of RTAΔm by ENGase occurs in *Ngly1*$^{-/-}$ MEF cells, it is not clear whether such deglycosylation could also proceed in endogenous substrates. Accordingly, cytosolic glycoproteins were detected by lectin staining using Concanavalin A (Con A) in different MEF cells in the presence of MG-132. While little difference in Con A staining between WT, *Ngly1*$^{-/-}$ and *Engase*$^{-/-}$ MEF cells was found, significantly higher levels of Con A-stained bands were observed for the cytosolic fraction of DKO MEF cells (**Figure 2.10**). Most of the Con A-stained bands disappeared in the case of PNGase F-treated samples, suggesting that the Con A-positive signals are derived from *N*-glycoproteins. Collectively, these findings indicate that ENGase-mediated deglycosylation may occur on ERAD substrates more frequently than originally thought.

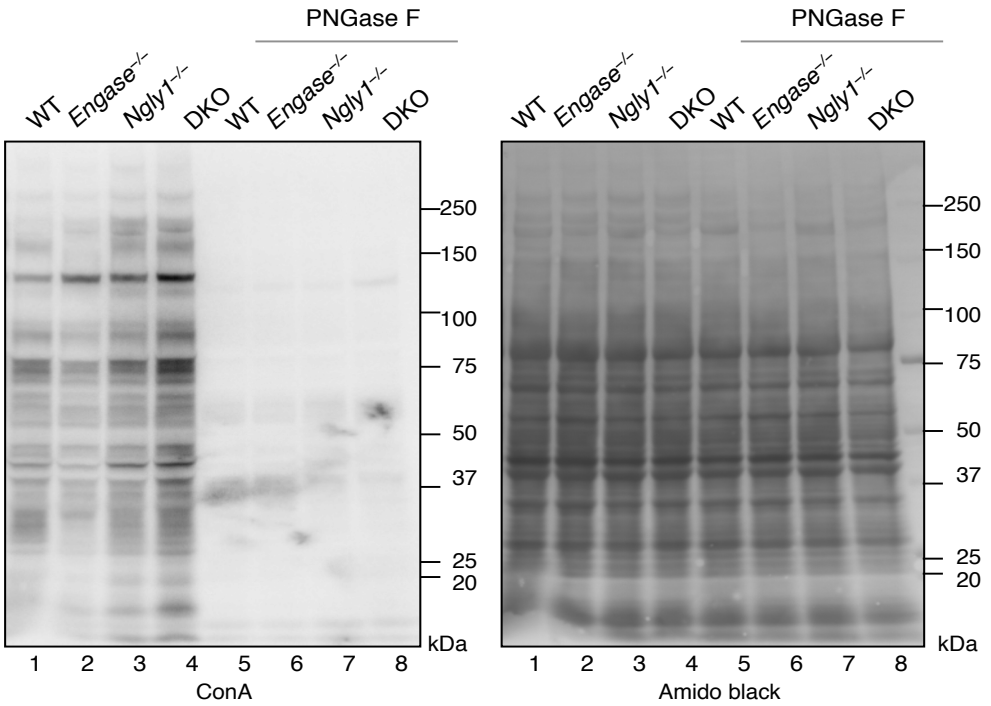

Figure 2.10. Con A staining of cytosolic extracts from WT, *Ngly1*$^{-/-}$, and *Engase*$^{-/-}$ and DKO MEF cells. Each lane contains 5 μg of cytosolic proteins. Lanes 1 to 4, cytosolic extraction of the four cell lines, lanes 5 to 8, PNGase F treated samples. Con A: lectin staining using Con A; Amido black; protein staining of the same membrane using Amido black.

Formation of Radioimmunoprecipitation assay buffer-insoluble RTAΔm is more pronounced in MEF cells expressing ENGase

While accumulation of the g0 form RTAΔm in the RIPA-insoluble fraction (RIF) was observed in ENGase-expressing DKO MEF cells, it was not certain whether this phenomenon is specifically caused by ENGase in cells lacking *Ngly1*. I therefore performed RIPA-extraction of RTAΔm from the WT, *Engase*$^{-/-}$, *Ngly1*$^{-/-}$, and DKO MEF cell lines. As shown in **Figure 2.11A**, the RIPA-insoluble g0 form was observed in

Ngly1$^{-/-}$ MEF cells, as well as in WT and *Engase*$^{-/-}$ MEF cells. However, the proportion of the g0 form of RTAΔm in RIF was significantly higher in *Ngly1*$^{-/-}$ MEF cells (91±7%) compared with other cells (**Figure 2.11B**). Moreover, the proportion in WT MEF cells (69±5%) was also found to be significantly higher when compared with *Engase*$^{-/-}$ MEF cells (29±10%) (**Figure 2.11B**). These results strongly suggest that the formation of the RIPA insoluble aggregate is more prominent in cells expressing cytoplasmic ENGase.

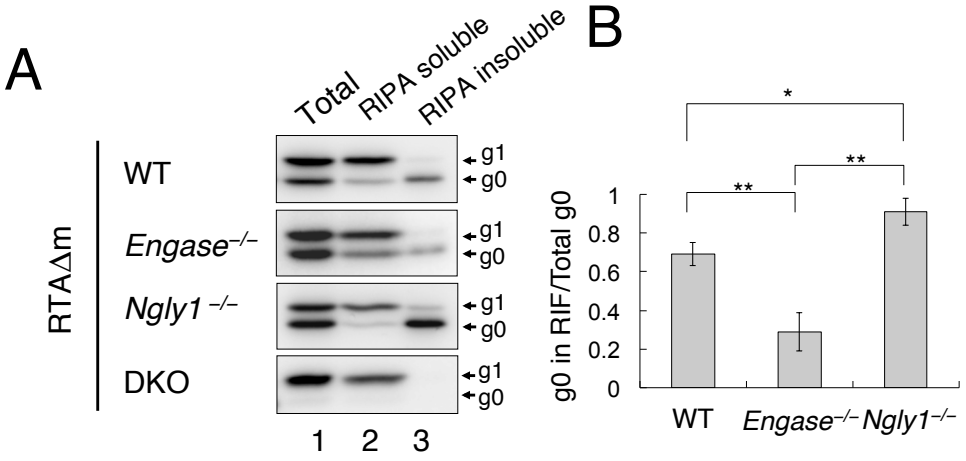

Figure 2.11. Non- or de-glycosylated RTAΔm are mainly recovered from RIPA insoluble fractions. (A) Separation of RIPA-soluble and RIPA-insoluble RTAΔm in WT, *Engase*$^{-/-}$, *Ngly1*$^{-/-}$, and DKO MEF cell lines. Cells expressing RTAΔm were extracted with SDS-PAGE sample buffer (lane 1, Total), RIPA buffer (lane 2, RIPA soluble), and the RIPA-insoluble fraction was solubilized with SDS-PAGE sample buffer (lane 3, RIPA insoluble). For each sample, an extract equivalent to ~5×10^4 cells was loaded. **(B)** Quantitation of RIPA-insoluble g0 in WT, *Engase*$^{-/-}$, and *Ngly1*$^{-/-}$ cells. RIF: RIPA-insoluble fraction. Data represents average ± SD of at least three independent samples. *: $p<0.05$; **: $p<0.01$ by Student's *t*-test.

RIPA-insoluble aggregates are stabilized in Ngly1$^{-/-}$ MEF cells

As RTAΔm is stabilized specifically in *Ngly1*$^{-/-}$ MEF cells during cycloheximide-decay analysis (**Figures 2.4C** and **D**), we speculated that in *Ngly1*$^{-/-}$ MEF cells, the RIPA insoluble RTAΔm aggregate is sequestered from proteasomal degradation. To address this issue, a cycloheximide-decay experiment of RTAΔm was performed using WT, *Ngly1*$^{-/-}$ and *Engase*$^{-/-}$ MEF cells, with RIPA soluble and insoluble fractions separated at 0, 1.5, and 3 h. As shown in **Figures 2.12A** and **B**, the accumulation of g0 RTAΔm in RIPA insoluble fraction of *Ngly1*$^{-/-}$ MEF cells was evident, when compared with *Engase*$^{-/-}$ or WT MEF cells. This result implies that deglycosylation by ENGase may change the soluble glycosylated RTAΔm into an aggregated g0 form. In contrast, we did not find an increase in the level of the RIPA insoluble g0 form in WT or *Engase*$^{-/-}$ MEF cells **(Figures 2.12A** and **B)**. These results indicate that the RIPA insoluble g0 form of RTAΔm formed in *Ngly1*$^{-/-}$ MEF cells is highly stable, while other g0 forms, *i.e*. nonglycosylated or PNGase-deglycosylated RTAΔm, did not appear to be stabilized.

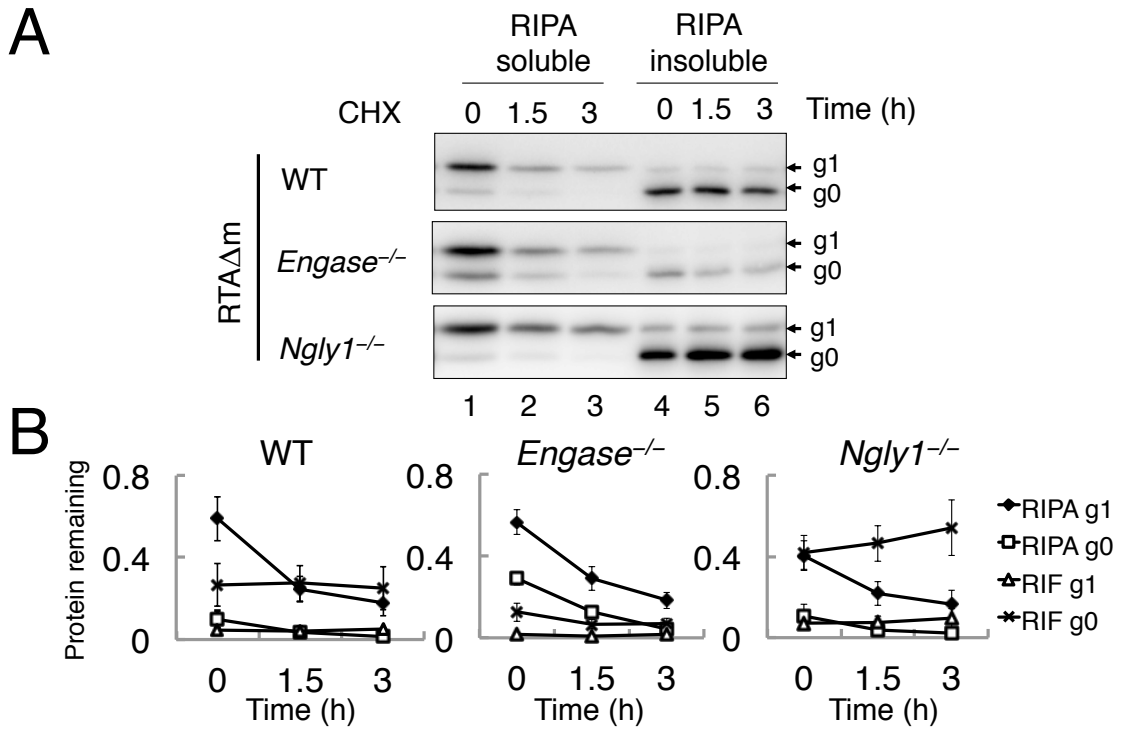

Figure 2.12. RIPA-insoluble proteins are stabilized in *Ngly1*$^{-/-}$ MEF cells. **(A)** Cycloheximide chase assay of RIPA soluble/insoluble RTAΔm in WT, *Ngly1*$^{-/-}$, and *Engase*$^{-/-}$ MEF cells. Cells expressing RTAΔm were chased using cycloheximide for the indicated time intervals. The RIPA soluble (lanes 1 to 3) and RIPA insoluble extracts (lanes 4 to 6) were assessed. For each sample, extracts equivalent to 5×10^4 cells were loaded. **(B)** Time course analysis of g1 and g0 levels in WT, *Ngly1*$^{-/-}$, and *Engase*$^{-/-}$ MEF cells. Data represents average ± SD of three independent samples.

Non-glycan form RTAΔ easily gets aggregated and stabilized in the cell

As the shown in **Figure 2.12** and **Figure 2.13**, the g0-RTAΔ in *Engase*$^{-/-}$ MEF cells, which is speculated to be generated by Ngly1, has less tendency to get aggregated and stabilized compared to the ENGase-generated *N*-GlcNAc modification containing g0-RTAΔ in *Ngly1*$^{-/-}$ MEF cells, it is questioned whether the *N*-GlcNAc modification causes the aggregation. To verify this, an RTAΔ mutant was constructed by changing the

remaining Asn *N*-glycosylation site to Asp in RTAΔm, which has the same amino acid sequence with the RTAΔm after the deglycosylation by PNGase. Another non-glycan mutant of RTAΔ, RTAΔ(N10Q/N236Q) with both Asn *N*-glycosylation sites changed to Gln, was also constructed to examined if there is any difference caused by the amino acid sequence. The clearance of the both mutants in RIPA-soluble and RIF fraction was detected in *Ngly1*$^{-/-}$ MEF cells. As shown in **Figure 2.13**, it is likely that RTAΔ is intrinsically prone to form aggregates which could be recovered in the RIF as long as there was no glycans attached to the protein (upper, lanes 7-9). It is therefore speculated that regardless of the presence of *N*-GlcNAc, aggregation of RTAΔ may impair the proteasomal degradation.

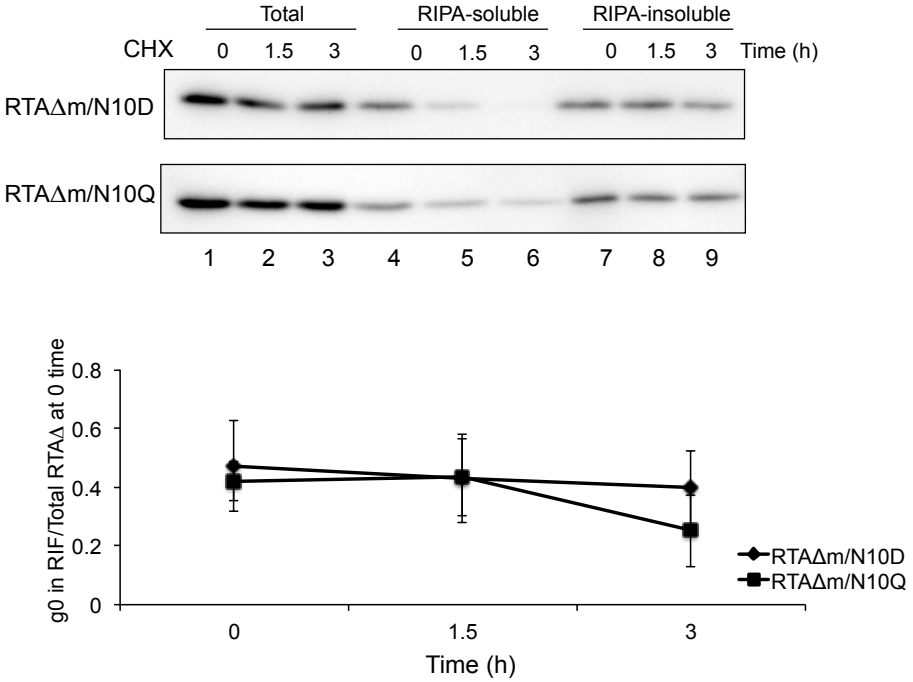

Figure 2.13 the expression of non-glycan form RTAΔ in *Ngly1*$^{-/-}$ MEF cell also causes the RIF aggregation which slowered the clearance of the protein. (A)

Cycloheximide chase assay of RIPA soluble/insoluble RTAΔm/N10D and RTAΔm/N10Q in *Ngly1*$^{-/-}$ MEF cells. Cells expressing RTAΔ mutant were chased using cycloheximide for the indicated time intervals. The RIPA soluble (lanes 4 to 6) and RIPA insoluble extracts (lanes 7 to 9) were assessed. For each sample, extracts equivalent to 5×10^4 cells were loaded. **(B)** Time course analysis of g0 levels in the RIPA insoluble fraction. Data represents average ± SD of three independent samples.

DISCUSSION

Since the identification of the gene encoding the cytoplasmic PNGase [28], several reports have demonstrated that this enzyme is indeed involved in the glycoprotein ERAD process[41, 43, 45, 47, 48, 54, 55, 56, 57, 58, 59, 60, 61, 63]. More recently, the *in vivo* deglycosylation has been detected by a very sophisticated assay system, using a model ERAD substrate that exhibits fluorescence in a deglycosylation-dependent manner[64]. It was also reported that the EDEM1 protein, a key component of the glycoprotein ERAD process, was stabilized upon the inhibition of cytosolic PNGase, implying that the EDEM1 may be the endogenous substrate for the PNGase[65]. No critical evidence, however, has been provided in terms of the biological significance of PNGase-mediated deglycosylation during the ERAD process in mammalian cells, as inhibition of PNGase activity did not cause the impairment of deglycosylation of EDEM1. In this study, we show in mammalian cells that Ngly1 is important for preventing ERAD substrates from forming mild detergent-insoluble aggregates. Using a new model ERAD substrate RTAΔm, ENGase was shown to act on misfolded glycoproteins in MEF cells lacking Ngly1, resulting in the generation of aggregation-prone *N*-GlcNAc modified proteins. Moreover, aggregates containing *N*-GlcNAc modified proteins were found to be significantly stabilized in *Ngly1*$^{-/-}$ MEF cells. Our results clearly indicate the functional importance of Ngly1 in the ERAD process, and further indicate a detrimental effect of ENGase, especially in the absence of Ngly1, on proper glycoprotein ERAD (**Figure 2.14**). It should also be noted that, based

on our current findings, to unequivocally confirm the action of Ngly1 on ERAD substrates *in vivo*, detecting deglycosylation by SDS-PAGE is not sufficient, and the introduction of negative charge(s) into the core peptide (*i.e.* the conversion of glycosylated Asn to Asp) should be independently confirmed, using methods such as isoelectoric focusing[48, 54].

To date, the direct action of cytoplasmic ENGase on glycoproteins has not been unequivocally demonstrated in mammalian cells. However, there is experimental evidence showing the intracellular occurrence of *N*-GlcNAc proteins, *i.e.* potential cytoplasmic ENGase reaction products, in murine synapses[66, 67, 68]. It was also clearly shown that at least some of the *N*-GlcNAc proteins are formed by the cytoplasmic ENGase activity in plants[51]. These results indicate that formation of *N*-GlcNAc proteins by ENGase may not be a rare event in cells. We therefore speculate that the action of ENGase may only be detrimental to a subset of glycoprotein ERAD substrates, especially in cells lacking *Ngly1*, thereby causing the formation of stable *N*-GlcNAc proteins.

A recent study has shown that the innermost GlcNAc on *N*-glycans may contribute to glycoprotein stability by forming stabilizing interactions between the GlcNAc and carrier proteins[69]. Therefore one can speculate that *N*-GlcNAc proteins may somehow affect the tertiary structure surrounding the glycosylation region and may lead to inefficient degradation by the proteasome. On the other hand, our study clearly showed that the tendency to be recovered in a RIPA-insoluble fraction is a general feature of nonglycosylated or deglycosylated RTAΔm, when compared with the *N*-glycosylated form (**Figure 2.11A**). This phenomenon may reflect the fact that, at least for RTAΔm,

attachment of a hydrophilic *N*-glycan may be critical in maintaining the solubility of the carrier protein. Consistent with this hypothesis, it is of interest to note that RTAΔm degradation in *Ngly1*$^{-/-}$*Engase*$^{-/-}$ DKO MEF cells is as efficient as in wild type, whereas its degradation remains to be proteasome-dependent. These observations further support the idea that, at least for RTAΔm, the efficiency of proteasomal degradation appears to be normal for *N*-glycan-containing proteins (which probably retain their solubility), even in the absence of Ngly1.

In *Engase*$^{-/-}$ MEF cells, it was found that minimal aggregate-formation is observed for the g0 form of RTAΔm (most likely the product of Ngly1). These results imply that, under physiological conditions, Ngly1-mediated deglycosylation and proteasomal degradation may be tightly coupled, so that the deglycosylated proteins undergo proteolytic degradation without forming aggregates. However, once this regulation is lost in *Ngly1*$^{-/-}$ MEF cells, detrimental aggregates may form. It should also be noted that, except in *Ngly1*$^{-/-}$ MEF cells, RIPA-insoluble RTAΔm does not seem to accumulate over time during cycloheximide decay experiments, implying that cells can somehow manage the aggregation-prone g0 forms, except the *N*-GlcNAc RTAΔm formed by the action of ENGase. The proportion of the RIPA insoluble RTAΔm g0 form appears to be considerably higher in WT MEF cells in comparison with *Engase*$^{-/-}$ MEF cells (**Figures 2.11A** and **B**), suggesting that ENGase-catalyzed deglycosylation may occur in WT MEF cells. However, this does not cause a delay in RTAΔm degradation (**Figures 2.4 C** and **D**), indicating that ENGase activity did not affect the overall efficiency of glycoprotein ERAD in WT MEF cells. It is therefore conceivable that the

effect of ENGase towards glycoprotein ERAD substrates is somehow more pronounced in the absence of Ngly1.

While Png1 mutants in budding yeast[28] or in plants[70] did not show any significant phenotypic consequences, more recent studies suggests that PNGase orthologue may play important physiological roles in other eukaryotes[29, 35, 71, 72]. Recent exome analysis studies have identified human patients with mutations in the *NGLY1* gene[36, 37]. These patients exhibited multiple symptoms that include developmental delay, multifocal epilepsy, involuntary movement, abnormal liver function, and absent tears. Currently, it is unclear how this observation correlates with our current finding, *i.e.* compromised degradation of RTAΔm caused by the RIPA insoluble aggregates in *Ngly1*$^{-/-}$ MEF cells. However, if the formation/aggregation of *N*-GlcNAc proteins could somehow be related to the various symptoms in *NGLY1* patients, it is tempting to speculate that inhibition of ENGase activity may serve as a therapeutic target for patients carrying mutations in the *NGLY1* gene.

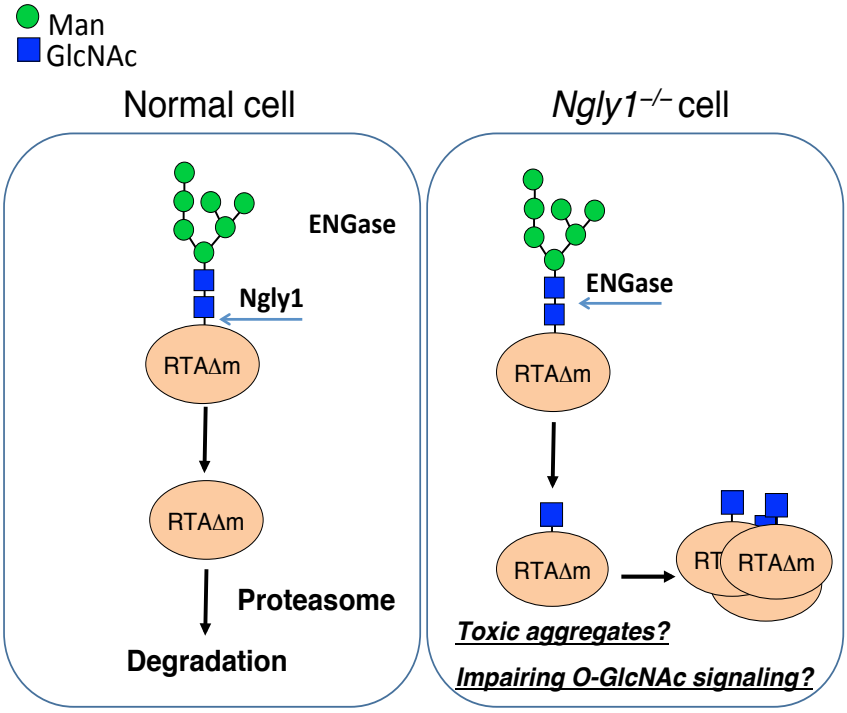

Figure 2.14. Schematic representation of ENGase-mediated formation of *N*-GlcNAc proteins in *Ngly1*$^{-/-}$ cells. (Left) In Ngly1+ cells, misfolded proteins like RTAΔm are deglycosylated predominantly by Ngly1 and are degraded efficiently by the proteasome; (Right) In the absence of Ngly1, ENGase acts on some portion of unfolded glycoproteins and makes *N*-GlcNAc proteins. Too much occurrence of *N*-GlcNAc proteins somehow causes detrimental effects on cells, possibly by an intrinsic toxicity of protein aggregates and/or impairment of intracellular signaling pathways involving *O*-GlcNAc.

EXPERIMENTAL PROCEDURES

Preparation of MEFs

MEF cells were established from fetuses of the *Ngly1*$^{-/+}$*Engase*$^{-/+}$ mice with a C57BL/6 congenic background (>96% isogenic for all MEF cells used) by Dr. Yoko Funakoshi (Glycometabolome Team), and the detailed procedure is described elswhere[73].

Cell cultures

MEF Cells were cultured in Dulbecco's modified Eagle's medium (Nacalai Tesque Co.) supplemented with 10% fetal bovine serum and antibiotics (100 units/mL penicillin G, 100 ng/mL streptomycin; Nacalai Tesque Co.) at 37°C in humidified air containing 5% CO_2.

Construction of plasmids

The GFP-encoding plasmid pEGFP-N1 was obtained from Clontech (Mountain View, CA). pcDNA-TCRα-HA was a generous gift from Dr. Yukiko Yoshida (Tokyo metropolitan institute of medical science)[56, 74]. pCMV-Tag4-NHK was a kind gift from Dr. Nobuko Hosokawa (Kyoto University)[75], and C-terminal V5-tag was added by site-directed mutagenesis using the following primers; NHK/pCMVV5-forward; 5'-CCTCTCCTCGGTCTCGATTCTACGTAGCTCGAGGATTACAAGGATGACG-3', and NHK/pCMVV5-reverse, 5'-ACCGAGGAGAGGGTTAGGGATAGGCTTACCTGCACGGCCTTGGAGAG-3'.

Ricin non-toxic A subunit RTA cDNA[44] was cloned into an ER retention plasmid pEF/*myc*/ER (Invitrogen) between the *Sal* I and *Not* I sites to establish pEF/RTAΔ/*myc*/ER. To construct pEF/RTAΔ/V5-*myc*/ER, a V5 tag was added before the *myc* tag at the *Not* I cleavage site by amplifying the pEF/RTAΔ/*myc*/ER plasmid using the V5-forward, 5'-CTAACCCTCTCCTCGGTCTCGATTCTACGGCCGCAGAACAAAAAC-3', and V5-reverse, 5'-GGAGAGGGTTAGGGATAGGCTTACCCCGTTTGATCTCGAGAAACT-3' primer pairs. Plasmids pEF/RTAΔN10Q/V5-*myc*/ER, pEF/RTAΔN236Q/V5-*myc*/ER, pEF/RTAΔN10QN236Q/V5-*myc*/ER, and pEF/RTADN10DN236Q/V5-*myc*/ER with point mutations on N10, N236, or both sites were generated from pEF/RTAΔ/V5-*myc*/ER using the following primer pairs: N10Q-forward, 5'-AAACAATACCCAATTATACAATTTACCACA-3', N10-reverse, 5'-TGGGTATTGTTTGGGGAATATCTG-3' for the N10Q mutation, and N236Q-forward, 5'-GACGTCAAGGTTCCAAATTCAGTGTGTACGA-3', N236Q-reverse, 5'-GAACCTTGACGTCTTTGCAGTTGAATTGGA-3' for the N236Q mutation, and N10D-forward; AAACAATACCCAATTATAGACTTTACCACA and N10-reverse; 5'-TGGGTATTGTTTGGGGAATATCTG-3' for N10D mutation. Total RNA was isolated from cells using the Qiagen RNEasy kit (Qiagen) from wild type MEF cells, and mouse cDNA was prepared from the total RNA using a SuperScript III RT kit (Invitrogen) according to the manufacturer's protocol. For construction of pcDNA3.1/ENGase/FLAG-His, ENGase cDNA was amplified using the following primers: ENGase-forward 5'-TATCCAGCACAGTGGCAGTCATGGAGACCTCGT-3' and ENGase-reverse 5'-

GTCGTCATCCTTGTAATCCTGAGGGACCGAGAAGAG-3'. The pcDNA3.1/V5-His backbone was amplified by pcDNA3.1-forward 5'-AAGGATGACGACGATAAGCGTACCGGTCATCATCAC-3', and pcDNA3.1-reverse 5'-GCCACTGTGCTGGATATCT-3'. These two DNA fragments were combined using an In-fusion HD cloning Kit (Clontech) according to the manufacturer's instructions. The FLAG peptide was divided into two parts and included on the ENGase-reverse primer and pcDNA3.1-forward primer, so that the V5 tag in the original pcDNA3.1/V5-His was replaced by a FLAG tag. All of the sequences were confirmed using PCR-based dideoxy termination methods using BigDye version 3.1 and a 3100 DNA sequencer (Applied Biosystems).

Plasmid transfection

Cells were transfected with plasmids using FuGENE HD transfection reagent (Roche Applied Sciences, Indianapolis, IN) according to the manufacturer's instructions. Briefly, 5×10^5 cells were seeded 12-16 h before transfection, and 1.5 μg plasmid/4.5 μL transfection reagent was mixed in 150 μL opti-MEM (Invitrogen) and incubated for 25 min before addition to the cultures. For co-transfection, 1 μg plasmid/3 μL transfection reagent was used for each plasmid. All the transiently transfected cells were incubated for 48 h before harvesting for analysis. For stable expression, *Ngly1*$^{-/-}$ MEF cells transfected with pEF/RTAΔN236Q/V5-*myc*/ER were maintained in medium supplemented with 0.8 mg/mL G418 (Nacalai Tesque Co.) for 7 days, and antibiotic resistant clones were isolated and RTAΔm expression was confirmed using western blotting.

Cycloheximide chase assay

Cells transiently transfected with pEF/RTAΔN236Q/V5-*myc*/ER were equally divided into six dishes 24 h after transfection (at 60% confluence), 50 μg/mL cycloheximide (Sigma, St. Louis, MO) was added to the cultures 48 h after transfection and the cells were collected at the indicated times. To inhibit proteasomal degradation, MG-132 (Peptide Institute Inc., Osaka, Japan) was added at final concentration of 5 μM upon addition of cycloheximide.

Cell lysis and western blotting

Cells were washed twice with PBS(-) buffer and dissolved in SDS-PAGE sample buffer (6.25 mM Tris-HCl pH 6.8, 2% SDS, 10% glycerol, 2.5% β-mercaptoethanol, 0.005% bromophenol blue) unless specified. For the isolation of RIPA buffer insoluble fractions, cells were lysed in RIPA buffer (25 mM Tris-HCl pH 7.4, 150 mM NaCl, 5 mM EDTA, 0.1% SDS, 1% TritonX-100, 0.5% sodium deoxycholate, 1 × compete protease inhibitor cocktail, 1 mM Pefabloc). After centrifugation at 15,000 × *g* at 4°C for 15 min, the supernatant was collected as the RIPA buffer soluble fraction, and the pellet collected as the RIPA buffer insoluble fraction, which were dissolved in SDS-PAGE sample buffer for SDS-PAGE and western blotting. For detecting RTAΔ, samples were transferred to polyvinylidene difluoride (PVDF) membranes (Millipore) and were incubated with anti-V5 antibody (Invitrogen; 1:5,000 in 5% skim milk/TBS-T), washed, and then incubated

with horseradish peroxidase (HRP)-conjugated anti-mouse IgG secondary antibody (Cell Signaling; 1:5,000 dilution). ENGase expression was detected using an anti-FLAG antibody (Sigma; 1:5,000 dilution) and anti-mouse IgG secondary antibody as described above. GFP was detected using an anti-GFP antibody (Invitrogen; 1:5,000) and anti-rabbit IgG (Cell Signaling; 1:5000 dilution) and the bands were detected by Immobilon Western Reagents (Millipore) and visualized using a FUJIFILM LAS-3000 mini, and the band intensity was quantitated using a MultiGauge V2.2 image reader.

Effect of MG-132 and lysosomal inhibitors on degradation of RTAΔm in DKO MEF cells

For the detection of proteasome-dependent degradation of RTAΔm, DKO MEF cells expressing with RTAΔm were evenly seeded to 6 dishes 24 h after the transfection of the plasmid, cycloheximide was added 24 h after the transfection, and cycloheximide was also co-incubated with the following reagents for 3 hours; 10 mM NH_4Cl (Nacalai Tesque Co.), 100 μM chloroquine (Sigma), the mixture of 2 μg/mL leupeptin (Peptide Institute Inc.) and 2 μg/mL pepstatain (Peptide Institute Inc.), or 5 μM MG-132 for 3 h before harvesting cells for analysis.

Extraction of the cytosolic proteins

Cells were collected after incubating with MG-132 for 4 h, washed three times with PBS, and resuspended with 800 μL of TNE buffer (25 mM Tris-HCl pH 7.4, 150 mM NaCl,

0.5 mM EDTA, 1× complete protease inhibitor cocktail (EDTA-free; Roche Applied Science), 1 mM Pefabloc (Roche Applied Science)), followed by homogenization in a motor-driven Potter-Elvehjem homogenizer. Debris was then cleared by centrifugation at 15,000 × *g* for 15 min at 4 °C, and the supernatant was further centrifuged at 100,000 × *g* for 60 min at 4°C to obtain the cytosol (supernatant) fraction. The protein amount was confirmed by Bio-rad protein assay kit with BSA as a standard, and 5 μg of the cytosolic protein was loaded for the Amido balck/Concanavalin A-staining analysis.

Amido black staining of the membrane and Concanavalin A (Con A) blotting

Cytosol fractions obtained as described above were separated by SDS-PAGE and transferred to a PVDF membrane before the blotting. The membrane was washed by deionized water (DIW) to get rid of the transfer buffer, and stained with amido black (0.5% amido black (Wako, Japan), 25% isopropanol, 10% acetic acid) for 6 s, followed by washing with DIW for 5 min to remove the excess dye. The image of the stained membrane was taken by a FUJIFILM LAS-3000mini, and the stained dye on the membrane was removed by washing with TBS-T buffer for 30 min. The destained membrane was further blocked with 10% BSA (Sigma) at 4°C overnight, and incubated with Con A-HRP (J-OilMills, Tokyo, Japan) for 6 h at 4°C. The membrane was then washed and the bands were detected by Immobilon Western Reagents (Millipore) and visualized using a FUJIFILM LAS-3000mini. For control of the ConA staining, same amount of each sample was denatured with 1% SDS and 0.25% β-mercaptoethanol at

100°C for 5 min, and incubated with PNGase F (Roche Applied Science) at 37°C for 4 h to remove the *N*-glycans.

Immunoprecipitation and mass spectrometry

Ngly1$^{-/-}$ MEF cells stably expressing RTAΔm were incubated in 5 μM MG-132 containing medium for 3 h, harvested and whole lysate from 4×10^7 cells was prepared in 1 mL of SDS-PAGE sample buffer. The extract recovered was diluted 10-fold with RIPA buffer and subjected to immunoprecipitation with 5 μL of mouse anti-V5 antibody (Invitrogen) and 50 μL of protein A agarose beads (GE Healthcare). Prior to the incubation with the antibody, incubation with protein A agarose beads was carried to pre-clear the samples. with After overnight rotation at 4°C, the beads were washed five times with RIPA buffer and the immunoprecipitated samples were separated by SDS-PAGE, and the bands on the SDS-PAGE gel were visualized using a silver stain MS kit (Wako Pure Chemical Industries) according to the manufacturer's instructions.

The mass spectrometry was performed by Dr. Naoshi Dohmae, Dr. Takehiro Suzuki (Collaboration Promotion Unit, RIKEN Global Research Cluster) and the detailed procedure is described elsewhere[73]. Briefly, the band corresponding to RTAΔm g0 was excised from the gel, and digested with sequencing grade TPCK-trypsin (Worthington Biochemical Co.) in 30 μL of digestion buffer (10 mM Tris-HCl, 0.05% decyl glucoside, pH 8.0) at 37°C for 12 h. The digest mixture was separated using a nanoflow LC (Easy nLC, Thermo Fisher Scientific) on an NTCC analytical column (C18, Φ0.075 × 100 mm,

3 μm, Nikkyo Technos Co., Ltd.) and subjected on-line to a Q-Exactive mass spectrometer (Thermo Fisher Scientific)[76].

Chapter 2. The involvement of autophagy in the catabolism of cytoslic free glycans

ABSTRACT

Macroautophagy plays a critical role in catabolizing cytosolic components via lysosomal degradation. Recent findings from our lab indicate that basal autophagy is required for the efficient lysosomal catabolism of sialyloligosaccharides, and that the down regulation of sialin, a lysosomal transporter of sialic acids can cause a significant delay in the cytosolic accumulation of such glycans. This chapter shows that the sialin protein level was increased when the autophagy process was inhibited. This effect appears to be specific to sialin, since the amount of LAMP1, another lysosomal membrane protein, remains constant under the same conditions. My results suggest that autophagy may regulate the stability of sialin, and it could lead to the cytosolic accumulation of sialyloligosaccharides in autophagy-defective cells.

INTRODCTION

The autophagy has been widely recognized as an important process for maintaining cellular homeostasis by delivering cytosolic components to lysosomes for degradation. It plays important roles in various processes such as self renewal, starvation/stress adaption, anti-bacteria invasion, and antigen-presentaion[7]. The autophagy has been divided into three classes, macroautophagy, microautophagy, and chaperone mediated autophagy. Among them, the macroautophagy is the major form and has been most extensively studied. During the macroautophagy process, a portion of the cytoplasm including soluble materials or organelles become sequestered within an isolation membrane to form double-membrane vesicles called 'autophagosomes', which later fuse with lysosome to form 'autolysosomes' for the final degradation of the contents within the autophagosomes[8, 77]. Herein, the macroautophagy is referred to autophagy for simplicity.

Autophagosome formation involves multiple, complex processes. Since the identification of the first autophagy related yeast gene *Atg1*[24, 78], the mechanism responsible for the formation of autophagosomes has been extensively studied[7, 77, 79]. Autophagy could be easily induced by a number of stimuli, including starvation or cellular stress. On the other hand, cellular components are also continuously catabolized by autophagy under normal, non-induced conditions, and this basal autophagy has been recognized as being critical for intracellular clearance[7].

It is well known that the glycosylation of proteins plays roles in various cellular phenomena in mammalian cells, including protein folding, the subcellular transport of

proteins, cell-cell interactions and development[80, 81]. In terms of the biosynthetic pathway for *N*-glycosylation, which is one of the common forms of glycosylation of proteins, almost all of the steps are now well understood. However, there are still outstanding questions that remain to be solved in terms of aspects of the degradation of *N*-glycoproteins. In particular, the non-lysosomal pathway for the degradation of proteins has not been well characterized. For instance, the intracellular accumulation of sialylated oligosaccharides derived from *N*-glycans have been observed in various cells and tissues[82, 83, 84, 85], while the catabolic pathway for these glycans remains unknown.

Recently in our lab, the attempts to clarify the catabolic pathway for glycoconjugates in mammalian cells has revealed the importance of basal autophagy in preventing the accumulation of sialyloligosaccharides in the cytosol[10]. Moreover, it was found that sialin, a lysosomal sialic acid transporter, was involved in the accumulation of sialyl fOSs in the cytosol by unknown mechanisms, as evidenced by the fact that the suppression of sialin expression resulted in a significant reduction in the levels of cytosolic sialyloligosaccharides[10] (Figure 3.1).

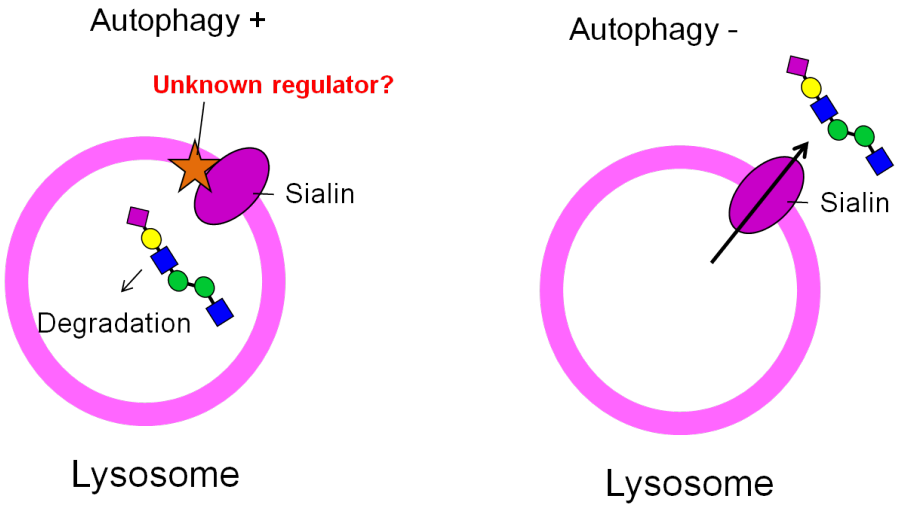

Figure 3.1. (Modified from ref. 10) Proposed mechanism for regulation of sialin-dependent export of sialyl-fOSs from the lysosome. A sialin molecule was shown to be involved to export sialyl-fOSs out of the lysosomes. (left) Complex type glycans including sialy-fOSs are degraded in the lysosomes in wild type cell with normal autophagy. An unknown regulator is possibly interacted with the sialin molecule to inhibit the export of the sialyl-fOSs to facilitate its degradation in the lysosomes. (right) Autophagy deficient cell loses such regulation, so that sialyl-fOSs may export out of the lysosome before its degradation.

The lysosomal membrane possesses various transporters for the export of degradation products formed within the lysosomes. As an anion transporter that exports sialic acid out of lysosomes, sialin was initially identified and has been widely studied due to the occurrence of sialic acid-storage disease that are caused by mutations in this gene[86, 87]. A wide range of substrates of sialin have been reported, including other anionic sugars, such as iduronic acid or glucuronic acid[4] as well as aspartate and glutamate[88, 89]. It has also been proposed that sialin is responsible for the synaptic or vesicular uptake of *N*-acetyl-

aspartylglutamate in neuronal cells[90]. Moreover, the structure-function study of sialin showed that a point mutant of sialin causes a dramatically different effect on the affinity as well as transport rate for sialic acid and glucuronic acid[91]. All of these reports point to a broad substrate specificity, as well as complex regulation, of this molecule under diverse conditions. The detailed mechanism responsible for how sialin is regulated by autophagy, however, remains to be elucidated.

RESULTS

Sialin is a multi-glycosylated membrane protein

To investigate the regulation of sialin by the autophagy process, m5-7 mouse embryonic fibroblast (MEF) cells was utilized. In these cells, the expression of *Atg5,* a gene essential for autophagosome formation, could be conditionally suppressed by the addition of doxycyclin (Dox)[92]. To detect the sialin molecule, mouse sialin with a V5 tag at the C-terminus was constructed. A previous study showed that the similar C-terminal tag of human sialin had negligible effect on its localization or its function[93]. In mammals, sialin is a multi-transmembrane protein containing seven consensus sequences for *N*-glycosylation, and human sialin was shown to be highly *N*-glycosylated[93]. Consistent with this observation, a western blotting analysis showed a diffuse band at a molecular mass of approximately 80 kDa, suggesting that the mouse sialin protein is also highly *N*-glycosylated (**Figure 3.2A**).

Since the heterogeneity in the size of proteins makes it difficult to quantitate the sialin content through western blotting analysis, the cell extracts were subjected to a PNGase F treatment prior to western blotting. As sialin-V5 was found to be unstable under prolonged incubation at 37°C (data not shown), the cell extracts were treated with PNGase F for different periods of time in order to find an optimal condition for the deglycosylation reaction. Sialin-V5 was shifted to a discrete band at a molecular mass of around 40 kDa after the PNGase F treatment (**Figure 3.2B**). To confirm that this band shift was not caused by degradation of the protein, a cell extract without PNGase F

treatment was subjected to a parallel incubation (**Figure 3.2B**, lanes 5-8), and no significant change in the staining pattern was observed. However, as the amount of detectable sialin-V5 was reduced after an incubation longer than 6 h (**Figure 3.2B** and data not shown), the PNGase F treatment was terminated after 4 h, to detect/quantitate the sialin-V5 proteins.

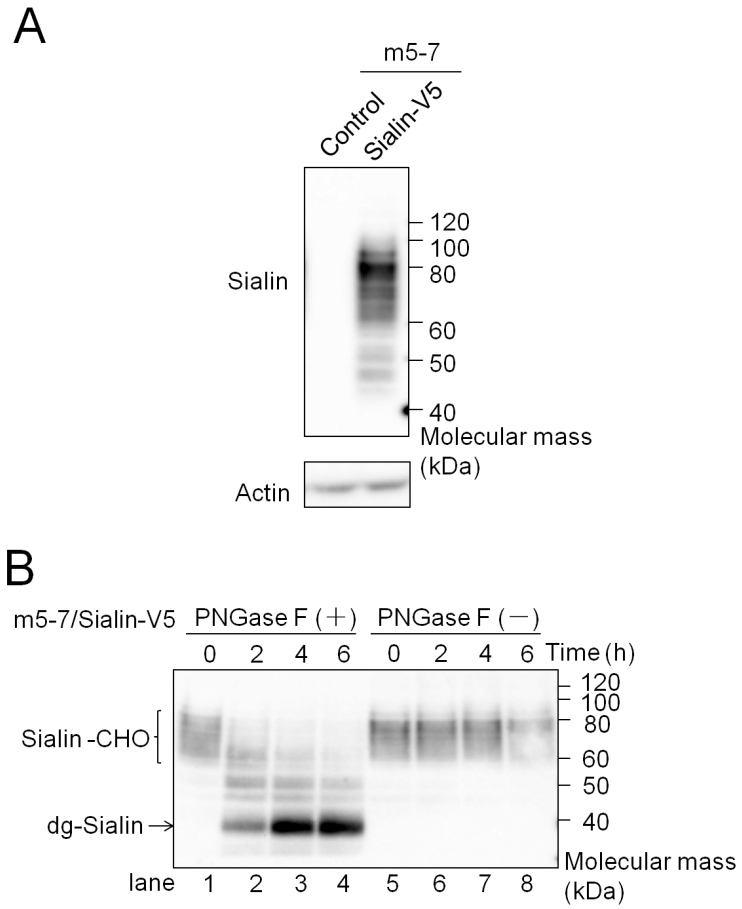

Figure 3.2. Sialin-V5 is expressed as a highly *N*-glycosylated protein in m5-7 MEF cells. (A) Western blotting analysis of sialin-V5 in m5-7 cells. Left, m5-7 cells expressing GFP (control); right, m5-7 cells expressing sialin-V5. The protein was detected by anti-V5 antibody. Actin was used as the loading control. **(B)** Lanes 1 to 4, western blotting pattern of sialin after PNGase F treatment for 0, 2, 4, and 6 h at 37 ºC;

lanes 5 to 8, 37 ºC incubation of the samples for 0, 2, 4, 6 h without addition of PNGase F. Sialin-CHO: glycosylated sialin, dg-sialin: deglycosylated sialin.

Sialin is stabilized under inhibition of autophagy

Having established a quantitation method for determining the amount of sialin-V5 proteins, the change in the amount of sialin was examined upon inhibition of the autophagy process. To this end, m5-7 cells expressing sialin-V5 were treated with Dox for the indicated times. The amount of sialin-V5 was increased upon the Dox treatment, suggesting that the protein level of sialin is, in fact, regulated by autophagy (**Figure 3.3A**, left, first panel). Interestingly, the levels of another lysosomal membrane protein, LAMP1, remained relatively constant during this treatment (**Figure 3.3A**, left, second panel). The impairment of autophagy process was confirmed by the disappearance of the LC3-II band (**Figure 3.3**A, left, third panel)[92]. Quantitation of each protein clearly indicated that sialin levels were increased upon impairment of the autophagy process (**Figure 3.3A**, right).

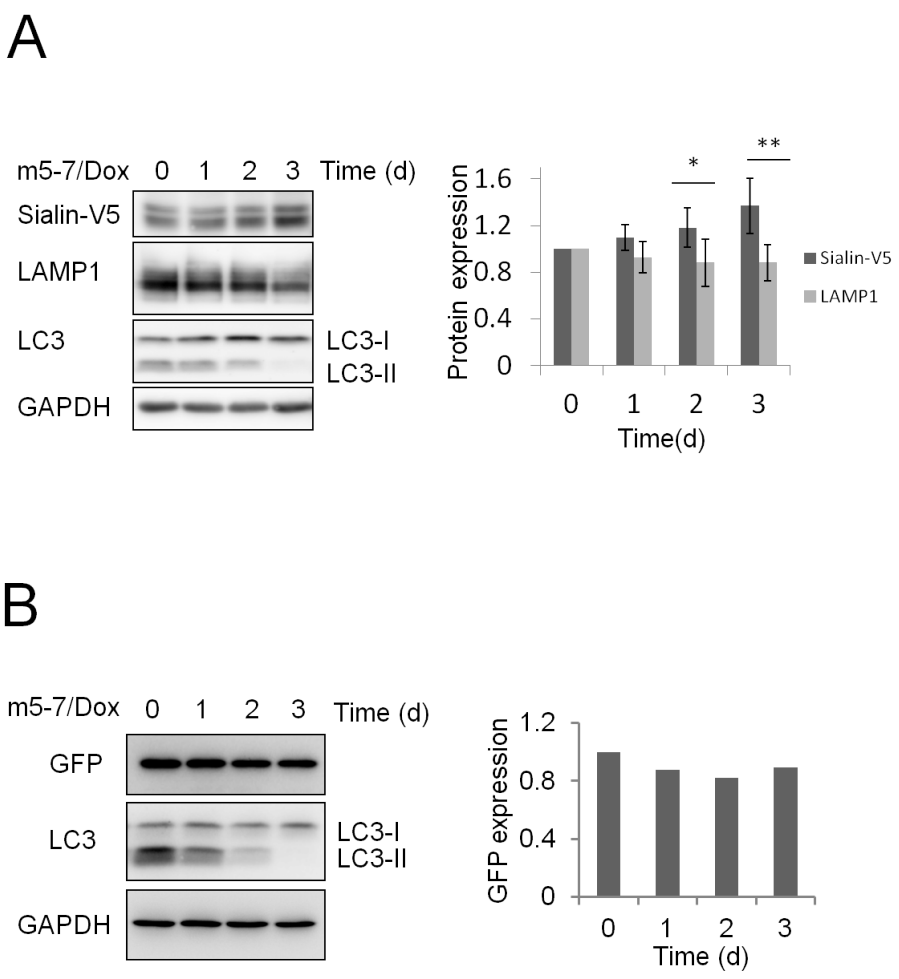

Figure 3.3. Sialin levels are increased upon the inhibition of autophagy, while amount of GFP expressed under the CMV promoter remained unchanged. (A) Left, sialin and LAMP1 expression in m5-7 cells treated with Dox (to shut down the expression of Atg5 protein critical for autophagosome formation) for 0, 1, 2, and 3 days. GAPDH was used as a loading control, and the defect of autophagosome formation was confirmed by the disappearance of LC3-II band. Right, quantification of the data shown in left. **(B)** Left, the expression of GFP, LC-3 and GAPDH in m5-7 cells under Dox-treatment for 0, 1, 2 and 3 days. Right, quantification of the data shown in left. Data was the relative amount of each protein normalized by the amount of GAPDH, and the protein amount of day 0 was set to 1. Error bars, S.D. from five independent experiments. *, $p < 0.05$; **, $p < 0.01$, student's *t*-test.

Because the sialin-V5 that I detected was exogenously expressed using the cytomegalovirus (CMV) promoter, it is still possible that the result could be an artifact for the protein expressed by the CMV promoter. To evaluate this possibility, GFP was expressed under the CMV promoter in m5-7 cells and the amount of GFP upon Dox treatment was examined. GFP protein expression was not increased at all under the same Dox treatment, suggesting that the increase in sialin protein levels under conditions of autophagy deficiency was not due to a general effect for proteins expressed under the CMV promoter (**Figures 3.3B**).

Morphological change of lysosomes was not observed upon shut-off of autophagy

Since the above findings clearly show that sialin levels are increased upon the inhibition of autophagy, the question arises as to whether such a change would affect the overall morphology of the lysosomes. To answer this question, m5-7 cells treated with or without Dox were fixed and LAMP1, a commonly used lysosomal marker, was stained with an anti-LAMP1 antibody. The inhibition of autophagy in the cells was confirmed by the disappearance of the LC3-II band (**Figure 3.4A**). The findings show that the overall morphology of lysosomes was not significantly changed, implying that the autophagic regulation of lysosomal protein is restricted to only a subset of proteins and does not influence the overall morphology of lysosomes (**Figure 3.4B**).

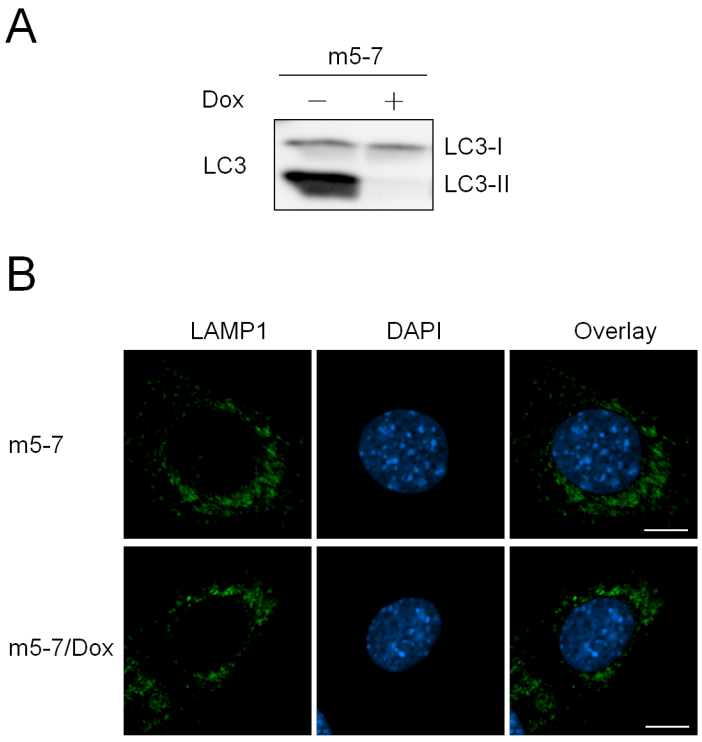

Figure 3.4. The morphology of lysosomes was not drastically altered upon the inhibition of autophagy. (A) Western blotting of m5-7 cells treated with (left), or without (right) Dox for 5 days. **(B)** Immunostaining of lysosomes with or without Dox treatment. m5-7 cells were treated with or without Dox for 5 days, followed by the staining with anti-LAMP1 antibody. Nuclei: DAPI (4',6-diamidino-2-phenylindole; blue), lysosomes: LAMP1 (green). Scale bar, 10 μm.

DISCUSSION

It has long been believed that autophagy is a process for delivering unwanted components for recycling. On the other hand, an emerging body of evidence shows the autophagy process can govern/control the function of lysosomes in diverse ways[94]. Previous study in our lab also showed that the basal autophagy process is critical for the normal lysosomal catabolism of sialyloligosaccharides, while the underlying mechanism responsible for this remains unclarified. My study provide convincing evidence to show that sialin protein levels are increased when the autophagy process is inhibited. It could be concluded that this effect is specific to sialin, since a corresponding increase was not observed for (1) LAMP1, another lysosomal membrane protein nor (2) GFP, a control protein expressed under the same CMV promoter.

The fact that the sialin in this study was not expressed by an endogenous promoter suggests that the increase in sialin protein levels under autophagy deficiency is most likely regulated at a protein level, *i.e.* in a post-translational manner. (**Figure 3.5**) The issue how an increase in the level of sialin has an impact on the catabolism of sialyloligosaccharides remains to be clarified. One obvious possibility is that, when the amount of sialin on lysosomal membranes is increased, the substrate specificity of sialin may somehow be affected, thus resulting in the premature release of sialyloligosaccharides, putative degradation intermediates, into the cytosol in autophagy-defective cells. Another more remote possibility is that, since autophagy is an important

process in clearing damaged lysosomes[94, 95], an autophagy-deficiency may lead to a malfunction of this process, leading to both an increase in sialin proteins and the release of sialyloligosaccharides into the cytosol, or in a defect in recovering these fOSs from the cytosol, for which these two events may not necessarily be correlated with each other. Nevertheless, the cytosolic accumulation of oligosaccharides in autophagy-defective cells exhibits a strict glycan specificity for sialylated oligosaccharides (*i.e.* not all-types of glycans were accumulated upon the inhibition of autophagy), implying that the effect is not merely due to an impaired lysosomal function. The findings also show that, under the experimental conditions employed in this study, no drastic change in the morphology of lysosomes was detected, suggesting that the effect is very specific to a subset of proteins, including sialin. Future studies will be needed to provide more insights into the connection between the increase of sialin levels and the accumulation of sialyloligosaccharides in the cytosol upon inhibiting the autophagy process.

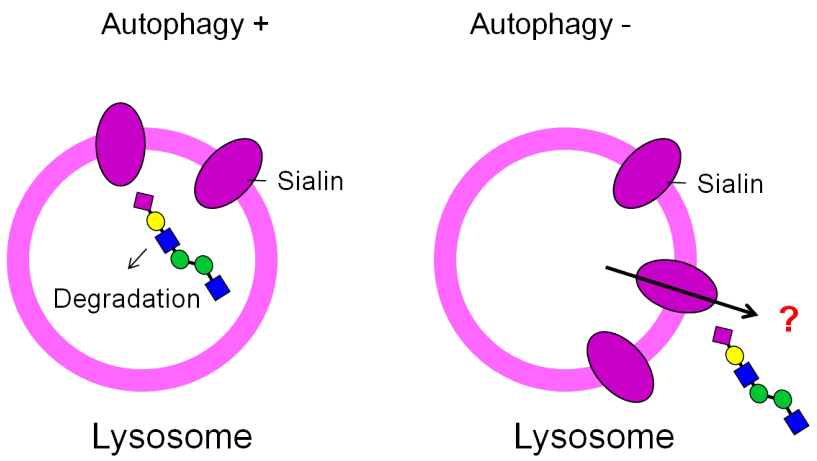

Figure 3.5. Proposed model for catabolism of sialyl-fOSs by autophagy process. The sialin molecule is stabilized upon the autophagy shut-off, thus resulted in a increased export of sialyl-fOSs to the cytosol before its degradation in the lysosomes.

EXPERIMENTAL PROCEDURES

Cell cultures

MEF m5-7 cells (Atg5 Tet-off plasmid in *Atg5*$^{-/-}$ background) were generously provided by Dr. Noboru Mizushima (The University of Tokyo, Japan). Cells were cultured in Dulbecco's modified Eagle's medium (Nacalai Tesque Co.) supplemented with 10% fetal bovine serum and antibiotics (100 units/mL penicillin G, 100 ng/mL streptomycin; Nacalai Tesque Co.) at 37ºC in humidified air containing 5% CO_2. Where indicated, 100 ng/mL doxycyclin (Dox, Sigma) was added to the culture medium.

Plasmid constructions

The GFP-encoding plasmid pEGFP-N1 was obtained from Clontech (Mountain View, CA). For the construction of pENTR-sialin, mouse cDNA was prepared from total RNA isolated from wild type MEF cells using Qiagen RNEasy kit (Qiagen), and the RNA was reverse-transcribed with random hexamers using a SuperScript III RT kit (Invitrogen) according to the manufacturer's protocol. Sialin cDNA was then amplified from the mouse total cDNA by the following primers: Sialin-forward 5'-CACCATGAGGCCCCTGCTTCGGG-3' and Sialin-reverse 5'-GTTTCTGTGTCCGTGGTGGTC-3'; and the amplified DNA fragment was cloned into the entry vector of the Gateway system, pENTR^{TM}/D-TOPO (Invitrogen). DNA sequences of the constructs were confirmed using PCR-based deoxy termination methods using BigDye ver. 3.1 and the ABI 3100 DNA Sequencer. To generate a vector

expressing C-terminal V5 epitope-tagged mouse sialin, the cDNA cloned into the entry vector was transferred into the destination vector (pcDNA^{TM}6.2/V5-DEST; Invitrogen) via LR clonase II reactions (Invitrogen) according to the manufacturer's instructions.

Plasmid transfection

Cells were transfected with plasmids using the FuGENE HD transfection reagent (Roche Applied Sciences, Indianapolis, IN) according to the manufacturer's instructions with optimized conditions. Briefly, 5×10^5 cells were seeded at a 6-cm dish 12-16 hours before transfection, and 1.5 μg of plasmids and 4.5 μL of transfection reagent was mixed in 150 μL opti-MEM (Invitrogen) and incubated for 25 minutes before adding to the cultures.

Cell lysis and western blotting

Cells were washed with PBS buffer (Nacalai Tesque Co.), and lysed in RIPA buffer (25 mM Tris-HCl pH 7.4, 150 mM NaCl, 5 mM EDTA, 0.1% SDS, 1% TritonX-100, 0.5% sodium deoxycholate, complete protease inhibitor cocktail (Roche Applied Sciences), 1 mM Pefabloc (Roche Applied Sciences)). After clearing the cell extracts at 15,000×*g* at 4ºC for 15 min, the supernatant was collected and was dissolved in SDS-PAGE sample buffer (6.25 mM Tris-HCl pH 6.8, 2% SDS, 10% glycerol, 2.5% β-mercaptoethanol, 0.005% bromophenol blue) before being applied for SDS-PAGE. For the deglycosylation of sialin, samples lysed in RIPA buffer, were treated with PNGase F (Roche) for the indicated times at 37°C before the addition of the SDS-PAGE sample buffer. After

separating the proteins by SDS-PAGE and transferring them to PVDF membranes (Millipore), the samples were subjected to western blotting analysis. For the detection of sialin, the membrane was incubated with an anti-V5 antibody (Invitrogen; 0.2 μg/mL), washed, and then incubated with an HRP-conjugated horse anti-mouse IgG secondary antibody (Cell Signaling; 1:5,000 dilution). LAMP1 was detected using an anti-LAMP1 antibody (Abcam; 0.2 μg/mL) and an HRP conjugated goat anti-rabbit IgG secondary antibody (Cell signaling; 1:5,000 dilution). GAPDH was detected using an anti-GAPDH antibody (Millipore; 1:5,000 dilution) and anti-mouse IgG (Cell Signaling; 1:5,000 dilution). Actin was detected using anti-actin antibody (Sigma; 0.15 μg/mL), and HRP conjugated anti-mouse IgG (1:10,000 dilution). Proteins of interest were detected by Immobilon Western Reagents (Millipore) and visualized using a FUJIFILM LAS-3000mini instrument (Fujifilm Co., Tokyo Japan). The band intensity was quantitated using a MultiGauge V2.2 image reader (Fujifilm Co., Tokyo Japan).

Immunofluorescence analysis

Cells grown on cover glasses (12-mm diameter) in a 24-well plate were washed with PBS pre-warmed at 37ºC, and fixed with 3% paraformaldehyde-PBS (PFA, Nacalai Tesque Co.) for 20 min. The cells were washed with PBS and excess PFA was quenched by adding 50 mM NH_4Cl for 10 min. After removing the NH_4Cl and washing with PBS, the cells were permeabilized by treatment with 50 μg/mL digitonin (Wako) for 10 min, they were washed, and then incubated in blocking buffer (1% BSA (Sigma) dissolved in PBS) for 30 min. Cells were incubated for at least 1 h with an anti-LAMP1 primary antibody

(Abcam, 2.5 μg/mL) in blocking buffer, washed with PBS and incubated with Alexa Fluor 488-conjugated goat anti-rabbit secondary antibody (Invitrogen, 2 μg/mL) in the same buffer for 1 h, washed with PBS and rinsed with water. The cells on the cover glasses were air dried and mounted on glass slides with MOWIOL (Kuraray Co. Ltd, Tokyo, Japan). For the staining of the nucleus, 4',6-diamidino-2-phenylindole (Invitrogen) was added together with the secondary antibody at a concentration of 10 μg/mL. Fluorescent images were acquired with a laser scanning confocal microscopy (FV500) (Olympus, Tokyo Japan) by a 60 × objective oil lens. The images were processed using FV10-ASW 4.0 viewer. Experiments were carried out at room temperature unless noted otherwise.

ACKNOWLEDGEMENTS

I give my deepest gratitude to my supervisor Dr. Tadashi Suzuki who taught me not only experimental details, and scientific interests, but also the value of the research, as well as the pride of a scientist in pursuing the truth. I appreciate his time spent with me, his encouragement and patient guidance have helped me to overcome many difficulties. Moreover, I am grateful to my co-supervisor Dr. Naoshi Dohmae, who patiently taught me knowledge about mass spectrometry. I would also like to show my gratitude to my co-supervisor Dr. Toshihisa Kotake who taught me the basic knowledge of glycobiology and offered me the great chance to make friends with other PhD students in Saitama University, and Dr. Yoichi Tsumuraya for his precious time to talk with me about the interest in research and plan in the future.

I am very grateful to Dr. Yoichiro Harada who taught me experiments, give me suggestions about experimental procedures, and discussed with me about the research plan. I appreciate his constant attention on my work and his encouragement very much. And I am very gratitude to Dr. Akira Hosomi, who give me suggestions for my experiment, talked with me about career plans and shared with me about his precious experiences. Also I am very grateful to Dr. Yoshimi Haga who taught me experiment procedures and design, gave me suggestions about my presentation and experiments, and she introduced me the Japanese cultures and made my early days in Japan easier. And I also would like to thank Dr. Li Wang, who gave me help in my experiment, helped me

whenever I have difficulty in my life or experiment, and encouraged me as a friend and senior. And I am also very thankful to Dr. Takehiro Suzuki and Ms. Akina Kawata for their help in MS analysis. Also I would like to thank Ms. Kumiko Ishii for her patient teach in the cell staining, and Dr. Takashi Angata, Dr. Shinobu Kitazume for their supports in my experiment, and also Dr. Yasuhiko Kizuka for his suggestions in my experiment.

I would like to thank Dr. Yoko Funakoshi, and Ms. Yuki Masahara-Negishi, and Dr. Fujihira Haruhiko for their wonderful discoveries in mouse study, as well as Mr. Junichi Seino who made the wonderful discovery in autophagy related project. I could never come to interesting findings without their finding, and I am also very thankful to Dr. Hiroto Hirayama for his help and suggestions in my experiment. And I would also like to thank Ms. Iida, Ms. Matsuda, and Ms. Tsuchiya for their support in my work.

Many thanks to Ms. Kotoko Ueno and Ms. Shinko Saito who helped with the administration and offered help in my life, and made my life in Japan easier. And I appreciate Dr. Ganesh Prasad Subedi for his help when I first came to Japan, and Mr. Tanim Jabid Hossain who shared his idea and his culture. And thanks to Dr. Shinya Hanashima, Ms. Akemi Ikeda, Ms. Kana Matsumoto, and Mr. Akitsugu Suga, I enjoyed the snowy mountain in Japan. And I am really grateful to all the members in systems glycobiology group, I had a colorful life because of them.

I would also thank my friends Hongna, Chunji, Xiaoyue, Tong, Sylvain and Jenney, who shared knowledge from different fields and spend these precious youthful days together with me in RIKEN. And special thanks to my friend for life, Tong Zhu, who is always there when I need audiences for presentations or any time when I need a help.

I would also like to express my gratitude to my former mentors Dr. Tatsuya Yamagata and Dr. Sadako Yamagata, as well as Dr. Takahisa Shinomiya, they showed me the amazing world of life science and teach me basic ideas about biological experiment, I appreciate every effort they did on me and I would never be able to continue my PhD work without their help.

And finally I would like to thank my families for their endless love and support across the sea.

REFERENCES

1. Kornfeld R, Kornfeld S. Assembly of asparagine-linked oligosaccharides. *Annu Rev Biochem* **54**, 631-664 (1985).

2. Herscovics A. Processing glycosidases of Saccharomyces cerevisiae. *Biochim Biophys Acta* **1426**, 275-285 (1999).

3. Herscovics A. Importance of glycosidases in mammalian glycoprotein biosynthesis. *Biochim Biophys Acta* **1473**, 96-107 (1999).

4. Winchester B. Lysosomal metabolism of glycoproteins. *Glycobiology* **15**, 1R-15R (2005).

5. Mellman I. Endocytosis and molecular sorting. *Annu Rev Cell Dev Biol* **12**, 575-625 (1996).

6. Luzio JP, Mullock BM, Pryor PR, Lindsay MR, James DE, Piper RC. Relationship between endosomes and lysosomes. *Biochem Soc Trans* **29**, 476-480 (2001).

7. Mizushima N. The pleiotropic role of autophagy: from protein metabolism to bactericide. *Cell Death Differ* **12 Suppl 2**, 1535-1541 (2005).

8. Yang Z, Klionsky DJ. Eaten alive: a history of macroautophagy. *Nat Cell Biol* **12**, 814-822 (2010).

9. Nascimbeni AC, Fanin M, Masiero E, Angelini C, Sandri M. The role of autophagy in the pathogenesis of glycogen storage disease type II (GSDII). *Cell Death Differ* **19**, 1698-1708 (2012).

10. Seino J, Wang L, Harada Y, Huang C, Ishii K, Mizushima N, Suzuki T. Basal autophagy is required for the efficient catabolism of sialyloligosaccharides. *J Biol Chem* **288**, 26898-26907 (2013).

11. Abraham D, Blakemore WF, Jolly RD, Sidebotham R, Winchester B. The catabolism of mammalian glycoproteins. Comparison of the storage products in bovine, feline and human mannosidosis. *Biochem J* **215**, 573-579 (1983).

12. Aronson NN, Jr. Aspartylglycosaminuria: biochemistry and molecular biology. *Biochim Biophys Acta* **1455**, 139-154 (1999).

13. Michalski JC, Klein A. Glycoprotein lysosomal storage disorders: alpha- and beta-mannosidosis, fucosidosis and alpha-N-acetylgalactosaminidase deficiency. *Biochim Biophys Acta* **1455**, 69-84 (1999).

14. Aronson NN, Jr., Kuranda MJ. Lysosomal degradation of Asn-linked glycoproteins. *FASEB J* **3**, 2615-2622 (1989).

15. Cacan R, Hoflack B, Verbert A. Fate of oligosaccharide-lipid intermediates synthesized by resting rat-spleen lymphocytes. *Eur J Biochem* **106**, 473-479 (1980).

16. Kmiecik D, Herman V, Stroop CJ, Michalski JC, Mir AM, Labiau O, Verbert A, Cacan R. Catabolism of glycan moieties of lipid intermediates leads to a single Man5GlcNAc oligosaccharide isomer: a study with permeabilized CHO cells. *Glycobiology* **5**, 483-494 (1995).

17. Moore SE, Bauvy C, Codogno P. Endoplasmic reticulum-to-cytosol transport of free polymannose oligosaccharides in permeabilized HepG2 cells. *EMBO J* **14**, 6034-6042 (1995).

18. Moore SE, Spiro RG. Intracellular compartmentalization and degradation of free polymannose oligosaccharides released during glycoprotein biosynthesis. *J Biol Chem* **269**, 12715-12721 (1994).

19. Suzuki T, Park H, Lennarz WJ. Cytoplasmic peptide:N-glycanase (PNGase) in eukaryotic cells: occurrence, primary structure, and potential functions. *FASEB J* **16**, 635-641 (2002).

20. Suzuki T, Funakoshi Y. Free N-linked oligosaccharide chains: formation and degradation. *Glycoconj J* **23**, 291-302 (2006).

21. Suzuki T, Hara I, Nakano M, Shigeta M, Nakagawa T, Kondo A, Funakoshi Y, Taniguchi N. Man2C1, an alpha-mannosidase, is involved in the trimming of free oligosaccharides in the cytosol. *Biochem J* **400**, 33-41 (2006).

22. Suzuki T. Cytoplasmic peptide:N-glycanase and catabolic pathway for free N-glycans in the cytosol. *Semin Cell Dev Biol* **18**, 762-769 (2007).

23. Kobata A. Exo- and endoglycosidases revisited. *Proc Jpn Acad Ser B Phys Biol Sci* **89**, 97-117 (2013).

24. Takahashi N. Demonstration of a new amidase acting on glycopeptides. *Biochem Biophys Res Commun* **76**, 1194-1201 (1977).

25. Plummer TH, Jr., Elder JH, Alexander S, Phelan AW, Tarentino AL. Demonstration of peptide:N-glycosidase F activity in endo-beta-N-acetylglucosaminidase F preparations. *J Biol Chem* **259**, 10700-10704 (1984).

26. Suzuki T, Seko A, Kitajima K, Inoue Y, Inoue S. Identification of peptide:N-glycanase activity in mammalian-derived cultured cells. *Biochem Biophys Res Commun* **194**, 1124-1130 (1993).

27. Suzuki T, Seko A, Kitajima K, Inoue Y, Inoue S. Purification and enzymatic properties of peptide:N-glycanase from C3H mouse-derived L-929 fibroblast cells. Possible widespread occurrence of post-translational remodification of proteins by N-deglycosylation. *J Biol Chem* **269**, 17611-17618 (1994).

28. Suzuki T, Park H, Hollingsworth NM, Sternglanz R, Lennarz WJ. PNG1, a yeast gene encoding a highly conserved peptide:N-glycanase. *J Cell Biol* **149**, 1039-1052 (2000).

29. Funakoshi Y, Negishi Y, Gergen JP, Seino J, Ishii K, Lennarz WJ, Matsuo I, Ito Y, Taniguchi N, Suzuki T. Evidence for an essential deglycosylation-independent activity of PNGase in Drosophila melanogaster. *PLoS One* **5**, e10545 (2010).

30. Kato A, Wang L, Ishii K, Seino J, Asano N, Suzuki T. Calystegine B3 as a specific inhibitor for cytoplasmic alpha-mannosidase, Man2C1. *J Biochem* **149**, 415-422 (2011).

31. Suzuki T, Yano K, Sugimoto S, Kitajima K, Lennarz WJ, Inoue S, Inoue Y, Emori Y. Endo-beta-N-acetylglucosaminidase, an enzyme involved in processing of free oligosaccharides in the cytosol. *Proc Natl Acad Sci U S A* **99**, 9691-9696 (2002).

32. Wang L, Suzuki T. Dual functions for cytosolic alpha-mannosidase (Man2C1): its down-regulation causes mitochondria-dependent apoptosis independently of its alpha-mannosidase activity. *J Biol Chem* **288**, 11887-11896 (2013).

33. Bernon C, Carre Y, Kuokkanen E, Slomianny MC, Mir AM, Krzewinski F, Cacan R, Heikinheimo P, Morelle W, Michalski JC, Foulquier F, Duvet S. Overexpression of Man2C1 leads to protein underglycosylation and upregulation of endoplasmic reticulum-associated degradation pathway. *Glycobiology* **21**, 363-375 (2011).

34. Thibault G, Ng DT. The endoplasmic reticulum-associated degradation pathways of budding yeast. *Cold Spring Harb Perspect Biol* **4**, (2012).

35. Habibi-Babadi N, Su A, de Carvalho CE, Colavita A. The N-glycanase png-1 acts to limit axon branching during organ formation in Caenorhabditis elegans. *J Neurosci* **30**, 1766-1776 (2010).

36. Enns GM, Shashi V, Bainbridge M, Gambello MJ, Zahir FR, Bast T, Crimian R, Schoch K, Platt J, Cox R, Bernstein JA, Scavina M, Walter RS, Bibb A, Jones M, Hegde M, Graham BH, Need AC, Oviedo A, Schaaf CP, Boyle S, Butte AJ, Chen R, Clark MJ, Haraksingh R, Cowan TM, He P, Langlois S, Zoghbi HY, Snyder M, Gibbs RA, Freeze HH, Goldstein DB. Mutations in NGLY1 cause an inherited disorder of the endoplasmic reticulum-associated degradation pathway. *Genet Med* **16**, 751-758 (2014).

37. Need AC, Shashi V, Hitomi Y, Schoch K, Shianna KV, McDonald MT, Meisler MH, Goldstein DB. Clinical application of exome sequencing in undiagnosed genetic conditions. *J Med Genet* **49**, 353-361 (2012).

38. Needham PG, Brodsky JL. How early studies on secreted and membrane protein quality control gave rise to the ER associated degradation (ERAD) pathway: the early history of ERAD. *Biochim Biophys Acta* **1833**, 2447-2457 (2013).

39. Aebi M, Bernasconi R, Clerc S, Molinari M. N-glycan structures: recognition and processing in the ER. *Trends Biochem Sci* **35**, 74-82 (2010).

40. Suzuki T, Harada Y. Non-lysosomal degradation pathway for N-linked glycans and dolichol-linked oligosaccharides. *Biochem Biophys Res Commun* **453**, 213-219 (2014).

41. Hirayama H, Hosomi A, Suzuki T. Physiological and molecular functions of the cytosolic peptide:N-glycanase. *Semin Cell Dev Biol*, doi:10.1016/j.semcdb.2014.11.009 (2014).

42. Suzuki T. The cytoplasmic peptide:N-glycanase (Ngly1)-basic science encounters a human genetic disorder. *J Biochem* **157**, 23-34 (2015).

43. Kim I, Ahn J, Liu C, Tanabe K, Apodaca J, Suzuki T, Rao H. The Png1-Rad23 complex regulates glycoprotein turnover. *J Cell Biol* **172**, 211-219 (2006).

44. Tanabe K, Lennarz WJ, Suzuki T. A cytoplasmic peptide: N-glycanase. *Methods Enzymol* **415**, 46-55 (2006).

45. Hosomi A, Tanabe K, Hirayama H, Kim I, Rao H, Suzuki T. Identification of an Htm1 (EDEM)-dependent, Mns1-independent Endoplasmic Reticulum-associated Degradation (ERAD) pathway in Saccharomyces cerevisiae: application of a novel assay for glycoprotein ERAD. *J Biol Chem* **285**, 24324-24334 (2010).

46. Hosomi A, Suzuki T. Cytoplasmic peptide:N-glycanase cleaves N-glycans on a carboxypeptidase Y mutant during ERAD in Saccharomyces cerevisiae. *Biochim Biophys Acta* **1850**, 612-619 (2014).

47. Blom D, Hirsch C, Stern P, Tortorella D, Ploegh HL. A glycosylated type I membrane protein becomes cytosolic when peptide: N-glycanase is compromised. *EMBO J* **23**, 650-658 (2004).

48. Hirsch C, Blom D, Ploegh HL. A role for N-glycanase in the cytosolic turnover of glycoproteins. *EMBO J* **22**, 1036-1046 (2003).

49. Misaghi S, Pacold ME, Blom D, Ploegh HL, Korbel GA. Using a small molecule inhibitor of peptide: N-glycanase to probe its role in glycoprotein turnover. *Chem Biol* **11**, 1677-1687 (2004).

50. Kato T, Kitamura K, Maeda M, Kimura Y, Katayama T, Ashida H, Yamamoto K. Free oligosaccharides in the cytosol of Caenorhabditis elegans are generated through endoplasmic reticulum-golgi trafficking. *J Biol Chem* **282**, 22080-22088 (2007).

51. Kim YC, Jahren N, Stone MD, Udeshi ND, Markowski TW, Witthuhn BA, Shabanowitz J, Hunt DF, Olszewski NE. Identification and origin of N-linked beta-D-N-acetylglucosamine monosaccharide modifications on Arabidopsis proteins. *Plant Physiol* **161**, 455-464 (2013).

52. Suzuki T. Introduction to "Glycometabolome" *Trends in Glycoscience and Glycotechnology* **21**, 219-227 (2009).

53. Suzuki T, Kwofie MA, Lennarz WJ. Ngly1, a mouse gene encoding a deglycosylating enzyme implicated in proteasomal degradation: expression, genomic organization, and chromosomal mapping. *Biochem Biophys Res Commun* **304**, 326-332 (2003).

54. Wiertz EJ, Jones TR, Sun L, Bogyo M, Geuze HJ, Ploegh HL. The human cytomegalovirus US11 gene product dislocates MHC class I heavy chains from the endoplasmic reticulum to the cytosol. *Cell* **84**, 769-779 (1996).

55. Hughes EA, Hammond C, Cresswell P. Misfolded major histocompatibility complex class I heavy chains are translocated into the cytoplasm and degraded by the proteasome. *Proc Natl Acad Sci U S A* **94**, 1896-1901 (1997).

56. Yu H, Kaung G, Kobayashi S, Kopito RR. Cytosolic degradation of T-cell receptor alpha chains by the proteasome. *J Biol Chem* **272**, 20800-20804 (1997).

57. Halaban R, Cheng E, Zhang Y, Moellmann G, Hanlon D, Michalak M, Setaluri V, Hebert DN. Aberrant retention of tyrosinase in the endoplasmic reticulum mediates accelerated degradation of the enzyme and contributes to the dedifferentiated phenotype of amelanotic melanoma cells. *Proc Natl Acad Sci U S A* **94**, 6210-6215 (1997).

58. Bebok Z, Mazzochi C, King SA, Hong JS, Sorscher EJ. The mechanism underlying cystic fibrosis transmembrane conductance regulator transport from the endoplasmic reticulum to the proteasome includes Sec61beta and a cytosolic, deglycosylated intermediary. *J Biol Chem* **273**, 29873-29878 (1998).

59. de Virgilio M, Weninger H, Ivessa NE. Ubiquitination is required for the retro-translocation of a short-lived luminal endoplasmic reticulum glycoprotein to the cytosol for degradation by the proteasome. *J Biol Chem* **273**, 9734-9743 (1998).

60. Petaja-Repo UE, Hogue M, Laperriere A, Bhalla S, Walker P, Bouvier M. Newly synthesized human delta opioid receptors retained in the endoplasmic reticulum are retrotranslocated to the cytosol, deglycosylated, ubiquitinated, and degraded by the proteasome. *J Biol Chem* **276**, 4416-4423 (2001).

61. Hirayama H, Suzuki T. Metabolism of free oligosaccharides is facilitated in the och1Delta mutant of Saccharomyces cerevisiae. *Glycobiology* **21**, 1341-1348 (2011).

62. Hirayama H, Seino J, Kitajima T, Jigami Y, Suzuki T. Free oligosaccharides to monitor glycoprotein endoplasmic reticulum-associated degradation in Saccharomyces cerevisiae. *J Biol Chem* **285**, 12390-12404 (2010).

63. Masahara-Negishi Y, Hosomi A, Della Mea M, Serafini-Fracassini D, Suzuki T. A plant peptide: N-glycanase orthologue facilitates glycoprotein ER-associated degradation in yeast. *Biochim Biophys Acta* **1820**, 1457-1462 (2012).

64. Grotzke JE, Lu Q, Cresswell P. Deglycosylation-dependent fluorescent proteins provide unique tools for the study of ER-associated degradation. *Proc Natl Acad Sci U S A* **110**, 3393-3398 (2013).

65. Park S, Jang I, Zuber C, Lee Y, Cho JW, Matsuo I, Ito Y, Roth J. ERADication of EDEM1 occurs by selective autophagy and requires deglycosylation by cytoplasmic peptide N-glycanase. *Histochem Cell Biol* **142**, 153-169 (2014).

66. Chalkley RJ, Thalhammer A, Schoepfer R, Burlingame AL. Identification of protein O-GlcNAcylation sites using electron transfer dissociation mass spectrometry on native peptides. *Proc Natl Acad Sci U S A* **106**, 8894-8899 (2009).

67. Trinidad JC, Barkan DT, Gulledge BF, Thalhammer A, Sali A, Schoepfer R, Burlingame AL. Global identification and characterization of both O-GlcNAcylation and phosphorylation at the murine synapse. *Mol Cell Proteomics* **11**, 215-229 (2012).

68. Trinidad JC, Schoepfer R, Burlingame AL, Medzihradszky KF. N- and O-glycosylation in the murine synaptosome. *Mol Cell Proteomics* **12**, 3474-3488 (2013).

69. Culyba EK, Price JL, Hanson SR, Dhar A, Wong CH, Gruebele M, Powers ET, Kelly JW. Protein native-state stabilization by placing aromatic side chains in N-glycosylated reverse turns. *Science* **331**, 571-575 (2011).

70. Diepold A, Li G, Lennarz WJ, Nurnberger T, Brunner F. The Arabidopsis AtPNG1 gene encodes a peptide: N-glycanase. *Plant J* **52**, 94-104 (2007).

71. Gosain A, Lohia R, Shrivastava A, Saran S. Identification and characterization of peptide: N-glycanase from Dictyostelium discoideum. *BMC Biochem* **13**, 9 (2012).

72. Seiler S, Plamann M. The genetic basis of cellular morphogenesis in the filamentous fungus Neurospora crassa. *Mol Biol Cell* **14**, 4352-4364 (2003).

73. Huang C, Harada Y, Hosomi A, Masahara-Negishi Y, Seino J, Fujihira H, Funakoshi Y, Suzuki T, Dohmae N. Endo-beta-N-acetylglucosaminidase forms N-GlcNAc protein aggregates during ER-associated degradation in Ngly1-defective cells. *Proc Natl Acad Sci U S A* **112**, 1398-1403 (2015).

74. Yoshida Y, Chiba T, Tokunaga F, Kawasaki H, Iwai K, Suzuki T, Ito Y, Matsuoka K, Yoshida M, Tanaka K, Tai T. E3 ubiquitin ligase that recognizes sugar chains. *Nature* **418**, 438-442 (2002).

75. Hosokawa N, Wada I, Hasegawa K, Yorihuzi T, Tremblay LO, Herscovics A, Nagata K. A novel ER alpha-mannosidase-like protein accelerates ER-associated degradation. *EMBO Rep* **2**, 415-422 (2001).

76. Doerr A. Targeting with PRM. *Nat Methods* **9**, 950 (2012).

77. Mizushima N, Komatsu M. Autophagy: renovation of cells and tissues. *Cell* **147**, 728-741 (2011).

78. Matsuura A, Tsukada M, Wada Y, Ohsumi Y. Apg1p, a novel protein kinase required for the autophagic process in Saccharomyces cerevisiae. *Gene* **192**, 245-250 (1997).

79. Mizushima N, Sugita H, Yoshimori T, Ohsumi Y. A new protein conjugation system in human. The counterpart of the yeast Apg12p conjugation system essential for autophagy. *J Biol Chem* **273**, 33889-33892 (1998).

80. Helenius A, Aebi M. Roles of N-linked glycans in the endoplasmic reticulum. *Annu Rev Biochem* **73**, 1019-1049 (2004).

81. Haltiwanger RS, Lowe JB. Role of glycosylation in development. *Annu Rev Biochem* **73**, 491-537 (2004).

82. Ohashi S, Iwai K, Mega T, Hase S. Quantitation and isomeric structure analysis of free oligosaccharides present in the cytosol fraction of mouse liver: detection of a free disialobiantennary oligosaccharide and glucosylated oligomannosides. *J Biochem* **126**, 852-858 (1999).

83. Ishizuka A, Hashimto Y, Naka R, Kinoshita M, Kakehi K, Seino J, Funakoshi Y, Suzuki T, Kameyama A, Narimatsu H. Accumulation of free complex-type N-glycans in MKN7 and MKN45 stomach cancer cells. *Biochem J* **413**, 227-237 (2008).

84. Yabu M, Korekane H, Takahashi H, Ohigashi H, Ishikawa O, Miyamoto Y. Accumulation of free Neu5Ac-containing complex-type N-glycans in human pancreatic cancers. *Glycoconj J* **30**, 247-256 (2013).

85. Yabu M, Korekane H, Hatano K, Kaneda Y, Nonomura N, Sato C, Kitajima K, Miyamoto Y. Occurrence of free deaminoneuraminic acid (KDN)-containing complex-type N-glycans in human prostate cancers. *Glycobiology* **23**, 634-642 (2013).

86. Adams D, Gahl WA. Free Sialic Acid Storage Disorders. In: *GeneReviews* (ed^(eds Pagon RA, Adam MP, Ardinger HH, al. e). 2010/03/20 edn. University of Washington, Seattle (1993).

87. Verheijen FW, Verbeek E, Aula N, Beerens CE, Havelaar AC, Joosse M, Peltonen L, Aula P, Galjaard H, van der Spek PJ, Mancini GM. A new gene, encoding an anion transporter, is mutated in sialic acid storage diseases. *Nat Genet* **23**, 462-465 (1999).

88. Miyaji T, Echigo N, Hiasa M, Senoh S, Omote H, Moriyama Y. Identification of a vesicular aspartate transporter. *Proc Natl Acad Sci U S A* **105**, 11720-11724 (2008).

89. Miyaji T, Omote H, Moriyama Y. A vesicular transporter that mediates aspartate and glutamate neurotransmission. *Biol Pharm Bull* **33**, 1783-1785 (2010).

90. Lodder-Gadaczek J, Gieselmann V, Eckhardt M. Vesicular uptake of N-acetylaspartylglutamate is catalysed by sialin (SLC17A5). *Biochem J* **454**, 31-38 (2013).

91. Courville P, Quick M, Reimer RJ. Structure-function studies of the SLC17 transporter sialin identify crucial residues and substrate-induced conformational changes. *J Biol Chem* **285**, 19316-19323 (2010).

92. Hosokawa N, Hara Y, Mizushima N. Generation of cell lines with tetracycline-regulated autophagy and a role for autophagy in controlling cell size. *FEBS Lett* **581**, 2623-2629 (2007).

93. Morin P, Sagne C, Gasnier B. Functional characterization of wild-type and mutant human sialin. *EMBO J* **23**, 4560-4570 (2004).

94. Shen HM, Mizushima N. At the end of the autophagic road: an emerging understanding of lysosomal functions in autophagy. *Trends Biochem Sci* **39**, 61-71 (2014).

95. Maejima I, Takahashi A, Omori H, Kimura T, Takabatake Y, Saitoh T, Yamamoto A, Hamasaki M, Noda T, Isaka Y, Yoshimori T. Autophagy sequesters damaged lysosomes to control lysosomal biogenesis and kidney injury. *EMBO J* **32**, 2336-2347 (2013).